AN INVESTIGATION ON MULTIBAND ULTRA-THIN POLARIZATION INSENSITIVE METAMATERIAL BASED MICROWAVE ABSORBER AND THEIR APPLICATION

A Thesis submitted in partial fulfillment of the requirement for the Award of the Degree of

MASTER OF ENGINEERING/MASTER OF TECHNOLOGY

in Electronics and Communication

Submitted By

MANPREET KAUR

Roll No.: 801761011

Under the Supervision of

Dr. Hari Shankar Singh

Assistant Professor, ECED

ELECTRONICS AND COMMUNICATION ENGINEERING DEPARTMENT

THAPAR INSTITUTE OF ENGINEERING AND TECHNOLOGY

(A DEEMED TO BE UNIVERSITY) PATIALA, PUNJAB

DECLARATION

I, **Manpreet Kaur** hereby declare that the work presented in this thesis entitled **"An Investigation on Multiband Ultra-Thin Polarization Insensitive Metamaterial based Microwave Absorber and their Application"** in partial fulfillment of the requirement for the award of degree of **Master of Engineering (ECE)** submitted at **Electronics and Communication Engineering Department**, Thapar Institute of Engineering & Technology (Deemed to be University), Patiala is an authentic record of work carried out under supervision of **Dr. Hari Shankar Singh (Assistant Professor, ECED, Thapar Institute of Engineering & Technology)** from 2018 to 2019. The matter presented in this has not been submitted either in part or full to any other university or institute for the award of any other degree.

Manpreet

Signature

Date: 5|8|19

(Manpreet Kaur)

(801761011)

Harishankar Singh

Dr. Hari Shankar Singh

Assistant Professor

Department of Electronics And Communication Engineering,

Thapar Institute of Engineering & Technology (A deemed To be University),

Patiala, 147001, Punjab, India.

Date: 05|08|2019.

ACKNOWLEDGEMENT

First of all, I express my sincere thanks to the all almighty God for honoring me with knowledge, intelligence, well-being, cognizance and the brainpower to conduct this research successfully.

I wish to express my deep gratitude and sincere thanks to my supervisor, **Dr. Hari Shankar Singh**, Assistant Professor, Electronics and Communication Department (ECED), Thapar Institute of Engineering and Technology, Patiala, for his invaluable guidance, constant encouragement, constructive comments, sympathetic attitude, and immense motivation, which has sustained my efforts at all stages of this work. His valuable advice and suggestions for the corrections, modifications and improvement did enhance my work.

I would like to express my gratitude to **Dr. Alpana Agarwal**, the head of Electronics and Communication Department (ECED), Thapar Institute of Engineering and Technology, Patiala, for providing me with adequate environment in carrying out the work. I am also thankful to the course coordinator, **Dr. Amit Mishra**, for his guidance about the work.

Finally, I want to extend my gratitude to all those persons who directly or indirectly helped me in carrying out this work in right direction.

Manpreet Kaur

ABSTRACT

A dual-band ultra-thin compact polarization-independent metamaterial absorber is proposed. The proposed absorber consists of two resonating structures i.e. a swastika-shaped and a square ring-shaped. The swastika-shaped structure is enclosed within a square ring. The size and thickness of the unit cell are 6×6 mm^2 and 0.015λ (where λ is the lowest resonating frequency), respectively. The combination of two resonating structures provides peak absorbance at 5.65GHz and 10.91GHz with maximum absorptivity 98.8% and 99.5%, respectively. The application platform of the reposed absorber lies in C and X band.

A compact ultrathin metamaterial absorber with three resonances in S-band, X-band and Ku-band is proposed. The geometry of the proposed absorber consists of a square ring, a split ring, and a plus-shaped resonating structure. The plus-shaped structure is enclosed within a split-ring resonator and it is further enclosed by an outer square ring. The proposed absorber is fabricated on a low-cost FR4 substrate of thickness 1mm i.e. 0.011 λ (where, λ is the lowest resonating frequency). The size of the unit cell size is 10×10 mm^2. It exhibits are 99.6%, 99.1%, and 99.1% absorption at 3.4 GHz, 9.6 GHz and 13 GHz, respectively.

Further, a wideband metamaterial absorber has been discussed in this thesis. The proposed structure consists of an L-shaped structure and a diagonal rectangular shaped structure. The dimension of the unit cell arrangement is 5×5 mm^2 and the thickness of the structure is 1.54 mm. The proposed structure provides the wideband absorptivity of 9 GHz from 12 GHz to 21 GHz having absorption of 99.6%, 99.9% and 97.6% at three resonating frequencies i.e. 12 GHz, 17 GHz and 21 GHz respectively.

Finally, a multiple-input multiple-output (MIMO) configuration planar inverted-F antenna (PIFA) has been presented for the use in mobile handsets with high isolation between the antenna elements. The isolation is enhanced by using an array of the metamaterial absorber between the antenna elements at a focused frequency of 5.65 GHz. The proposed antenna elements geometry consists of swastika-shaped design on the FR-4 substrate having dimensions of $7 \times 7 \times 0.8$ mm^3 at a height of 2.8mm from the ground plane of dimensions $100 \times 50 \times 0.8$ mm^3. An array of 4×4 unit cells of metamaterial absorber is used to enhance isolation between the antenna elements. Results show that the isolation between the antenna elements has improved from -12dB to -25dB at the operating frequency of 5.65 GHz. Further, S-parameters, radiation characteristics, and diversity parameters are analyzed.

TABLE OF CONTENTS

LIST OF ABBREVIATIONS

SRR	Split Ring Resonator
ELC	Electric Field Driven LC
RCS	Radar Cross Section
TE	Transverse Electric Mode
TM	Transverse Magnetic Mode
MIMO	Multiple Input And Multiple Output
PIFA	Planar Inverted-F Antenna

LIST OF TABLES

LIST OF FIGURES

CHAPTER 1
INTRODUCTION

1.1 METAMATERIAL

A metamaterial is a kind of material that exhibits a property not found in natural materials. They are the materials which are made by the composition of metals or plastics thus involving the assemblies of different elements. Metamaterials can modify the incoming electromagnetic wave in different ways such as absorbing, blocking, enhancing, or bending the wave due to their smart properties like compact size, shape, unique geometry, orientation, and arrangement to achieve an advantage over the conventional materials [1]. Moreover, metamaterials exhibit properties like negative permittivity and negative permeability which are not found in ordinary materials.

The metamaterial [2], being an unnatural structure has gained attentiveness in various fields like negative refraction [3], perfect lens [4], cloaking [5], antenna size shrinking [6] and many more due to its various distinctive properties. Absorbers are a type of metamaterial practiced to eliminate stray or undesirable radiation that could intervene in the working of the system. In the past few years, metamaterial absorbers due to their various advantages over standard absorbers such as perfect absorption, compact size, and ultra-thin thickness have been used as a substitute for the usual absorbers in the microwave, terahertz and infrared regions [7-9]. Several metamaterial absorbers have been developed and studied which are made of different attributes, such as solo band, double band, tri-band, four-band and wideband. Various metamaterial applications can be done in the frequency bands of the microwave region which are listed below in Table 1.1. Initially, split ring resonator (SRR) based metamaterial absorbers were used but nowadays electric field-driven LC (ELC) based metamaterial geometries are chosen, which results in thin absorber structures as the incoming electromagnetic wave need to cover much smaller distance in electric field-driven LC (ELC) based metamaterial geometries as compared to the split ring resonator (SRR) [10] based metamaterial geometries. Moreover, the initial designs were not suitable for many applications as they have been polarization-dependent means their absorption varies with the polarization angle. Further, they also exhibit very small bandwidth due to the resonating nature of the metamaterial geometries. But with the arrival of recent practical usage in radar cross-section (RCS) size shrinking of airplanes and other vehicles, shield from the intervention of electromagnetic waves [11–13], many types of research have been carried till date to include the above three attributes in one absorber geometry.

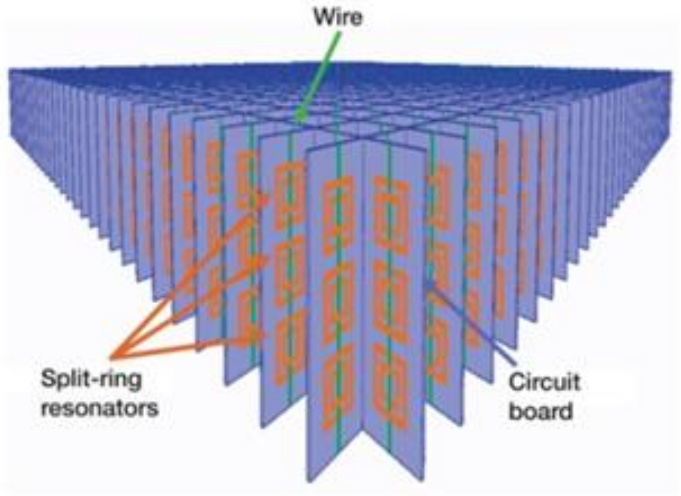

Figure 1.1 Metamaterials

The basic frequency bands of the microwave region are listed in Table 1.1.

Table 1.1 Frequency Bands

Frequency band	Frequency range (GHz)	Wavelength range (cm)
L-band	1-2	15-30
S-band	2-4	7.5-15
C-band	4-8	3.75-7.5
X-band	8-12	2.5-3.75
Ku-band	12-18	1.67-2.5
K-band	18-27	1.11-1.67
Ka-band	27-40	0.75-1.11
V-band	40-75	0.4-0.75
W-band	75-110	0.27-0.4

Metamaterials are known as the negative index materials as they consist of negative permittivity and negative permeability which further leads to the negative refractive index. They are also categories as left-handed media, media having a negative refractive index. These materials are also termed as double negative metamaterials or double negative materials (DNG).

Moreover, when the wave propagates to the fore direction then both permittivity ε and permeability μ are positive. When the backward wave is formed then both permittivity ε and permeability μ are negative and thus metamaterials are also known as backward wave media. When no-wave propagates then it means the permittivity ε and permeability μ are having different polarities. All these four cases are shown in Figure 1.2.

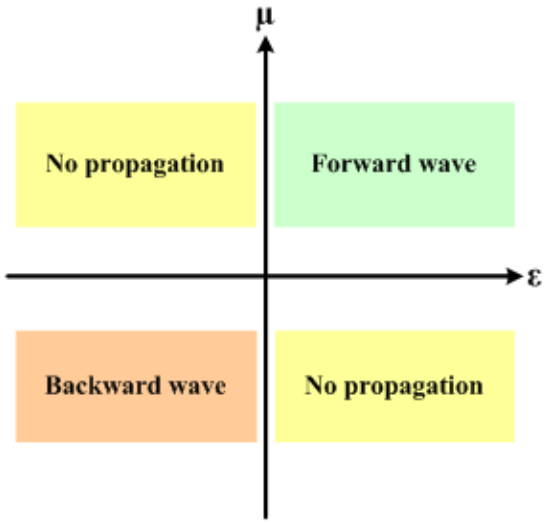

Figure 1.2 Different cases of wave propagation

1.2 APPLICATIONS OF METAMATERIALS

The followings are some approaching applications of metamaterial:

a) Antennas: Antennas which increases the miniaturized (electrically small) antennas performance by making the uses of artificial materials i.e. metamaterials. Their main function along with any antenna is to instigate the electromagnetic energy into the free environment. Further, metamaterial due to its novel structure is superior to its authentic size up to a great extent because of the reason of its capability to store and re-radiates energy. Therefore, the metamaterial can be employed as ultimately antenna/radiators miniaturization [6].

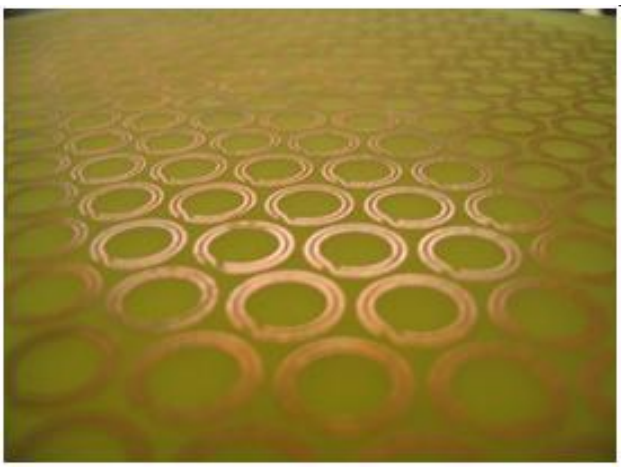

Figure 1.3 Metamaterial antenna

b) Absorbers: Another potential application of the metamaterials is as microwave absorber which attenuates the energy in an electromagnetic wave. Absorbers are a type of metamaterial practiced to eliminate stray or undesirable radiation that could intervene in the working of the system. Moreover, they are used externally as well as internally to diminish the reflection from the entity or the transmission from one entity to the other and to diminish the oscillations induced by the cavity resonance. Further, metamaterial absorbers eliminate the reflections in an anechoic chamber [14] thus creating a free space environment within the chamber. In the past few years, metamaterial absorbers due to their various advantages over standard absorbers such as perfect absorption, compact size, and ultra-thin thickness have been used as a substitute for the conventional absorbers. Several metamaterial absorbers have been developed and studied which are made of different attributes, such as single band, dual-band, the triple-band, quad-band and wideband. Thus, it is concluded that the metamaterial based microwave absorbers provide miniaturized structure, broader adaptability, and increased productiveness.

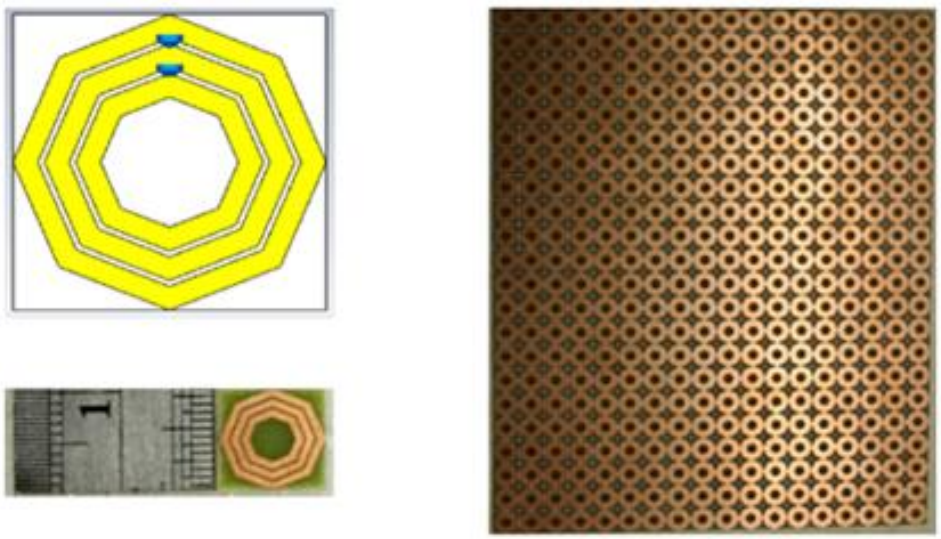

Figure 1.4 Metamaterial absorber

c) Super lens: Super lens makes the use of metamaterial to go ahead of the diffraction bound. The diffraction bound is a special attribute of conventional lenses and microscopes that bounds the fineness of their resolution[4].

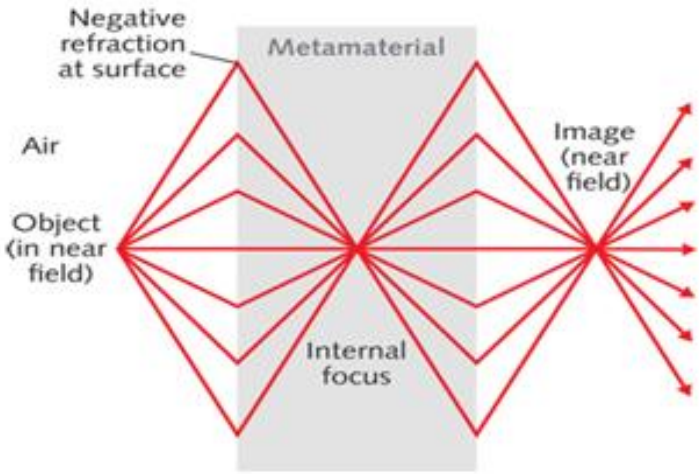

Figure 1.5 Metamaterial superlens

d) Cloaks: In metamaterial cloaking, the metamaterial is used is in an invisibility cloak. This is accomplished through a novel optical material by handling the paths travel across by the light. Metamaterial handles the propagation and transmission of particular parts of the light spectrum and directs the light. Further, metamaterial reveals the potential to deliver an object seemingly invisible. Based on transformation optics, metamaterial cloaking narrates the process of protecting something from view by handling the electromagnetic radiation [5].

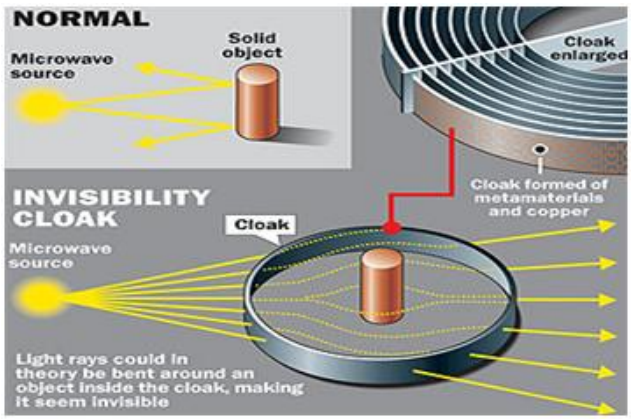

Figure 1.6 Metamaterial cloak

e) Sensors: Metamaterial being a non-natural media, flaunt improvement and tough localization of fields which further helps in improving the sensitivity and resolution of sensors because of its size which is scaled smaller than the wavelength of an outer stimulus. There are varieties of metamaterial sensors that can be used for a specific application. These sensors are biosensors (microwave, terahertz), thin-film sensors, wireless strain sensors, and many more.

Moreover, to monitor the non-invasive blood glucose, a microwave sensor based on the fake transmission line is used. The resultant numerical model shows the extent of the sensor which leads to the sensitivity suitable for monitoring the exact amount of glucose in the blood.

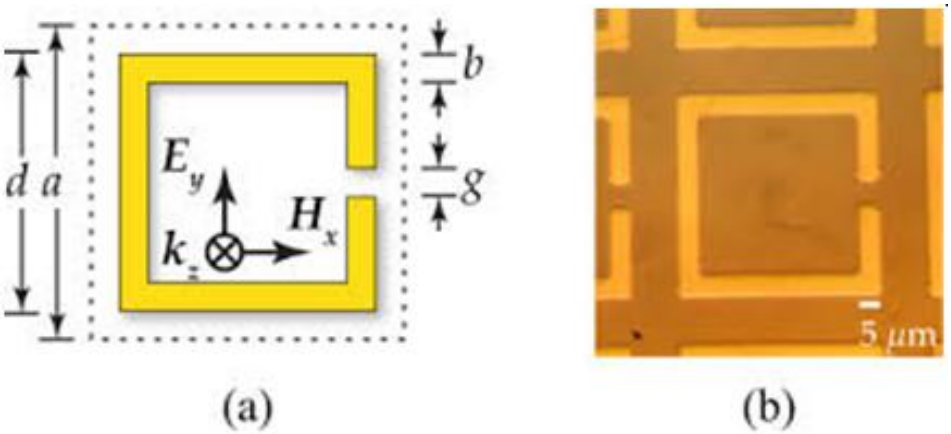

Figure 1.7 Metamaterial sensor

1.3 METAMATERIAL ABSORBERS

Absorption is highly required for different practices like energy harvesting, wave scattering reduction and many more. So, metamaterials with perfect absorption nearly 100% are designed to use in different applications. Thus, metamaterial absorbers have gained significant importance in the past few years due to their enormous property of absorbing the electromagnetic waves. A metamaterial absorber is a multi-layer structure or we can say that it is a sandwich-like structure in which most of the cases dielectric substrate is sandwiched in between the pattern formed of metal and the highly conducting metallic ground. Several metamaterial absorbers having multiple bands and broad bands that have been presented to date. Metamaterial absorbers with multiple band are designed using multiple resonating structures and when these multiple peaks come closer to each other the metamaterial absorber with a broader response is achieved.

In the electromagnetic wave, permittivity is the consequence of the electric field module while the permeability is the consequence of the magnetic field module.

The permittivity is in the form of composite term and is generally written as:

$\varepsilon^* = \varepsilon' - j\,\varepsilon''$

The dielectric polarization of the substance results in the emergence of the permittivity. The quantity ε’ is termed as the dielectric constant which changes considerably with the change in frequency. The quantity ε” is a count of the attenuation of the electric field triggered by the object.

The magnetic permeability is defined as:

$\mu^* = \mu' - j\,\mu''$

The permeability is a count of the material's upshot on the magnetic field. In the case of absorbers, permittivity and permeability both vary considerably over a small frequency range as they are the functions of frequency.

The permittivity has unit farads/meter and the permeability has unit henrys/meter. The value of permittivity and permeability in vacuum are:

$\varepsilon_0 = 8.854 \times 10^{-12}$ farads / meter and $\mu_0 = 4\pi \times 10^{-7}$ henrys / meter

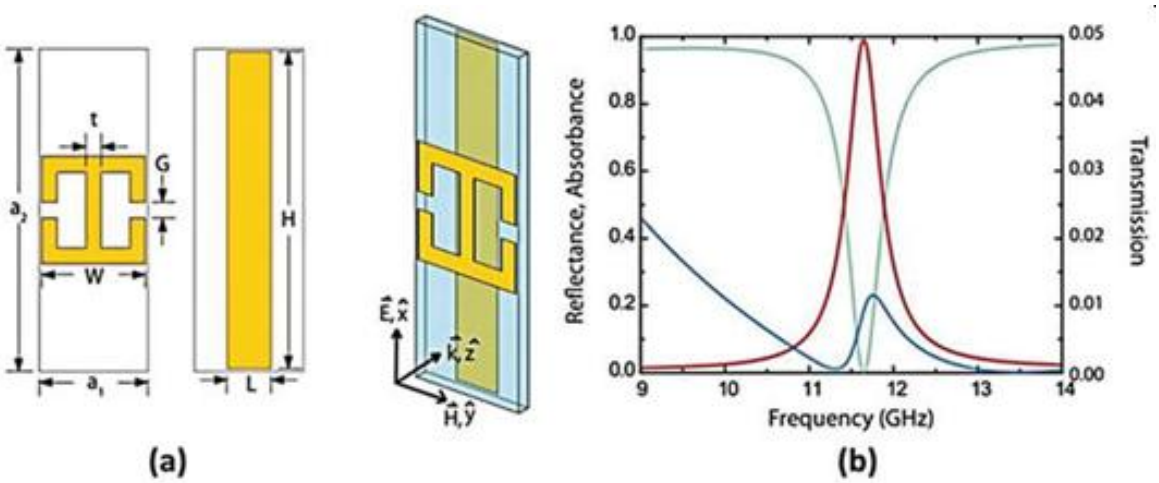

Figure 1.8 Metamaterial absorber

1.4 ABSORBER FORMS

a) Magnetic: Magnetic absorbers provide excessive permeability and excessive magnetic loss as they make use of a filler having ferromagnetic properties. Magnetic absorbers can largely compress the wavelength because of high permeability. Moreover, the magnetic field has the highest value on the conducting surface where the absorber is placed so they can be used for cavity resonance damping. Magnetic absorbers have the disadvantage of weight and cost but they are effortless to a machine and used in load applications. Different elastomer forms of magnetic absorbers include silicone, urethane, nitrile, and neoprene. They are also available in the rigid epoxy form.

Figure 1.9 Magnetic elastomer absorber

b) Dielectric: Dielectric absorbers have the value of permeability μ=1 because they have no magnetic properties. Dielectric absorbers have purely dielectric losses that can arise from different sources within the dielectric. Dielectric absorbers have lightweight and low cost and can also be used with elastomers. Dielectric absorbers due to the lack of magnetic absorption are not able to give good performance in the majority cavity resonance applications.

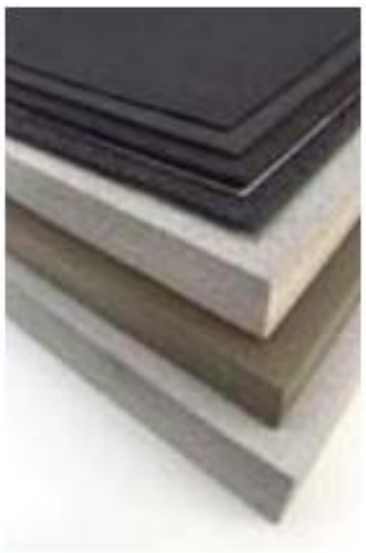

Figure 1.10 Range of dielectric form absorbers

c) Moldable: Moldable absorbers can be a two-division liquid which cures at room or elevated temperatures as well as can be in the variety of injection moldable pellets. Moreover, magnetic absorbers and dielectric absorbers both are present in moldable forms.

1.5 APPLICATIONS OF MICROWAVE ABSORBER

a) Near field absorbers: This is the category of absorbers that are positioned on or near the radiating component. Every design consists of elements like inductors, capacitors or connecting wires that can resonate and radiate at certain frequencies or behave differently at certain frequencies. Near field, absorbers contain excessive magnetic permeability and excessive magnetic loss as the energy in the near field is predominantly magnetic so radiators are formed as in the shape of a loop antenna. This magnetic energy fades away with the increase in the distance but can still intervene with the close by components. Near field, modeling comprises a loop antenna and a test antenna and coupling to the test antenna which is also a loop antenna is determined. Then the absorber is positioned in contact with the loop antenna to compare the coupling.

b) Loads: Microwave terminations are employed in the microwave systems like couplers or circulators to block the unwanted rays. Absorber load materials which are generally the magnetic absorbers are used so the termination ought to be proficient to absorb the incident energy and these load materials are easily molded or machined. Load absorbers are shaped as tapers so that they must absorb the entire waveguide band.

Figure 1.11 Load absorbers

c) Reflection reduction: Any system experiences the reflection which comes back to the transmitter whenever it transmits energy. Moreover, some unwanted reflections from other sources also interfere with the system. Thus, absorbers are used to reduce these reflections from the same source or different sources. Typically weather-resistant outdoor absorber can reduce reflection up to -20dB which can eliminate up to 99% of the reflection.

d) Radar cross-section reduction (RCSR): Absorbers can furthermore be utilized to diminish the radar cross-section of a mark. As the absorbers are used to reduce the reflections, thus reducing the reflection level results in a smaller cross-section, therefore absorbers are used to diminish the radar cross-section.

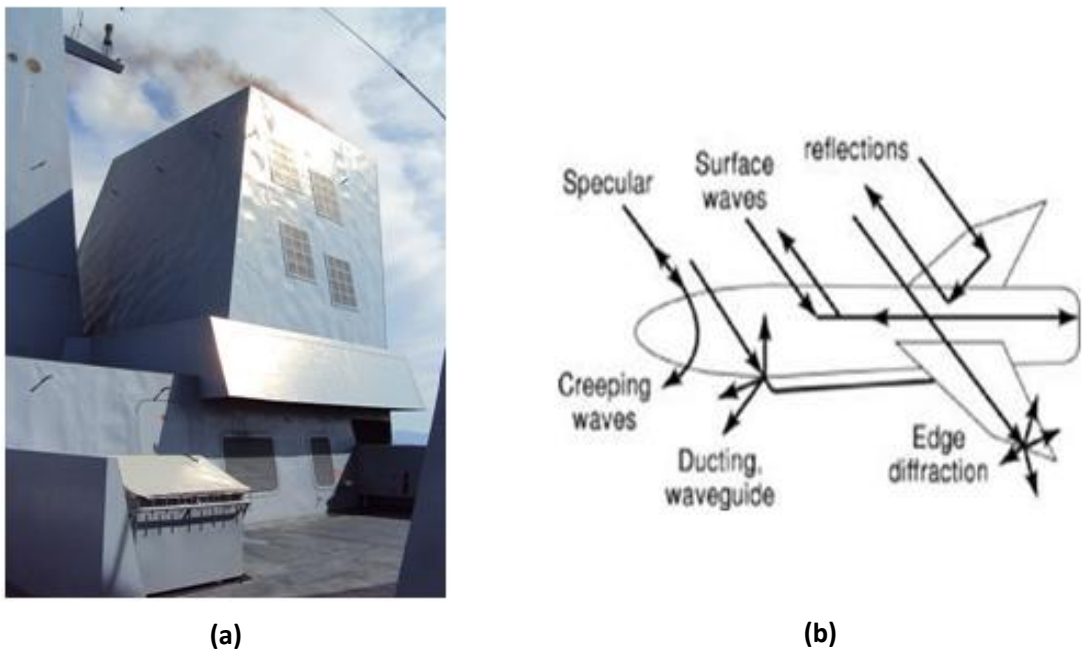

(a) **(b)**

Figure 1.12 (a) Radar cross-section reduction for stealth, (b) Scattering mechanism of the target

e) Antenna isolation: The use of multiple-input and multiple-output antennas in the wireless communication systems improves their performance and channel capacity but due to the space limitation in the wireless devices these antenna elements need to be closely spaced which results in the mutual coupling between these antenna elements which further led to the unwanted interference between the antennas. This mutual coupling also results in the reduction of their efficiencies as some part of their energy would be radiated to the other coupled antenna. So it's very important to provide proper isolation between these antenna elements. One of the methods to improve isolation between the antennas is to limit the radiation in the propagating direction and to increase the distance between the antennas. However, this method is not so efficient as the antenna elements have a very small area in mobile devices. Several other methods have also been proposed to provide isolation between the antenna elements but all these techniques are suitable for MIMO antennas with a common ground plane. To isolate the feeding port of closely packed antennas, multiple slits are etched on a single ground plane. Another technique includes two antennas that are connected with a so-called neutralization line to increase the port to port isolation. Another technique that

provides the isolation between the antenna elements without the need for a shared ground plane is the use of double negative metamaterial absorbers unit cell array. This technique provides the proper isolation between the antenna elements by preventing the coupling between the elements within the closely packed space of the mobile devices.

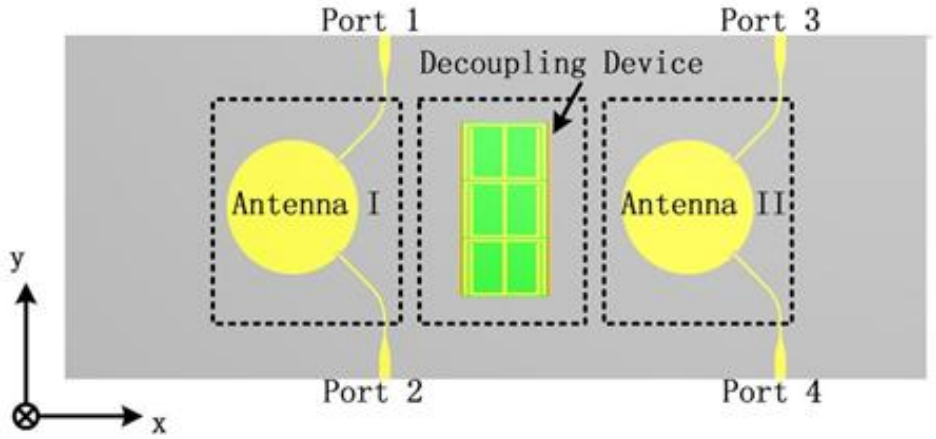

Figure 1.13 Dual-polarized patch antenna array with decoupling design

1.6 PLANAR INVERTED-F ANTENNA (PIFA)

Antenna inventors are all the time engaged in looking for different customs to advance the antenna's performance. One of them is to formulate the planar inverted-F antenna known as PIFA antenna which is progressively more used in the mobile phone trade. PIFA antenna introduces a shorting pin touching the patch and the ground plane and due to this PIFA antenna resonates at a one-fourth wavelength and thus covering the small space on the mobile phones. The PIFA antenna is so named as the planar inverted-F antenna due to its resemblance with inverted-F shape. This PIFA antenna gets so famous as a consequence of its compact size and omnidirectional pattern.

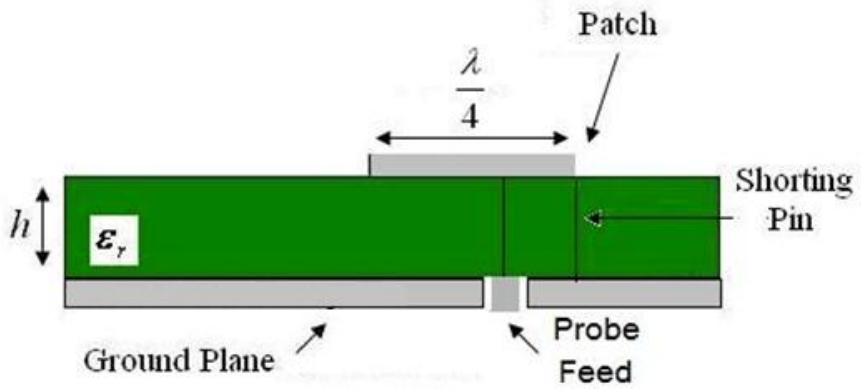

Figure 1.14 Planar inverted-F antenna (PIFA)

The feed point is put inside the open end and the short end due to the shorting pin and the input impedance is controlled by its position. In PIFA antennas, the shorting pin can also be a plate of any width.

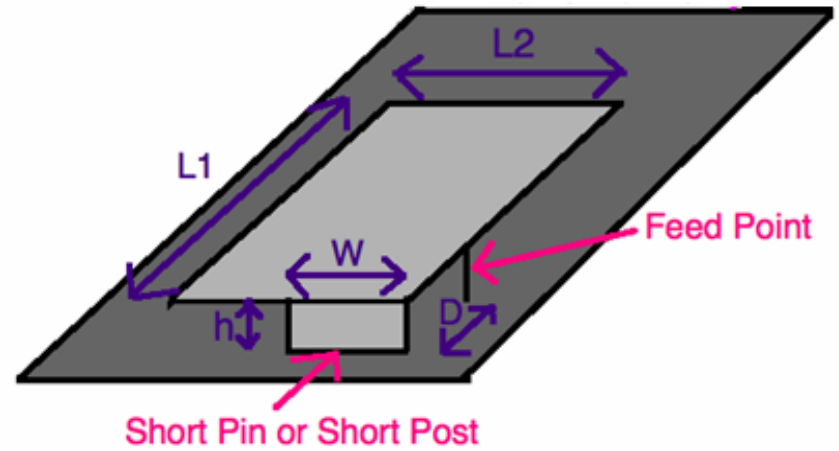

Figure 1.15 Planar inverted-F antenna (PIFA) with a shorting plate

The above Figure 1.15 shows that the planar inverted-F antenna (PIFA) consists of a patch of length L1 and width L2 which is placed at a height h from the ground surface, a feed point which is at a distance D from the short pin or short post. The shorting pin is placed at one edge of the antenna made of width W. The PIFA antenna impedance varies with the distance of the feed point from the shorting pin i.e. D in the above figure. When the feed point is made closer to the shorting pin, the impedance of the PIFA will reduce while the impedance of the PIFA can be improved by increasing the distance linking the short pin and the feed point.

Further, the length of the PIFA antenna can be reduced by using a capacitive loading technique in the PIFA antennas. In this method, the capacitance is added in the center of the feed point and the open edge.

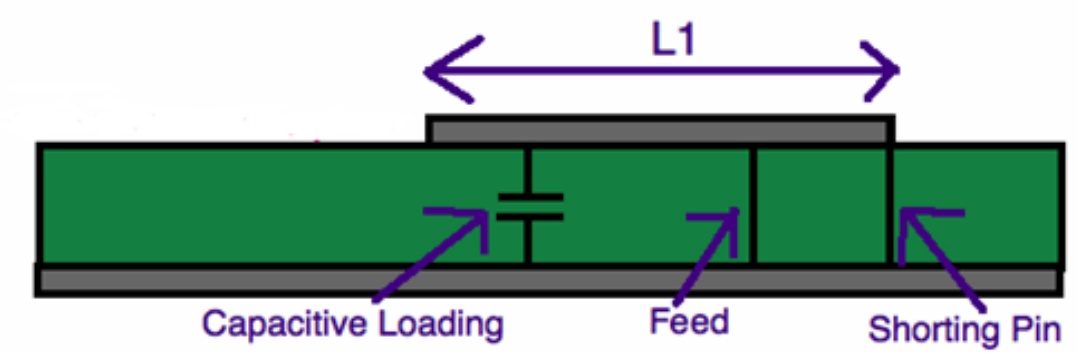

Figure 1.16 Capacitive loading in the planar inverted-F antenna (PIFA)

CHAPTER 2
LITERATURE SURVEY, RESEARCH GAPS, AND OBJECTIVES

2.1 LITERATURE SURVEY

The first aim is to study the research papers that have been already performed by the researchers. The research papers that are related to this thesis title are studied and their objectives and research gaps have been noted. Various developments in the past related to metamaterial absorbers and PIFA are studied and discussed in this chapter.

M. H. Li *et al.*, 2010 [15], presented a twice band metamaterial absorber showing results in the microwave area. The design has two ideal absorption curves at 11.15 GHz and 16.01 GHz which are shown by the simulated and experimental results. Absorptions are measured under different polarization angles of the electromagnetic waves with an extent of over 97% absorption at lower resonating frequency and 99% absorption at higher resonating frequency. Moreover, at different incident angles ranging from 0^o to 60^o, the absorption curves of the proposed metamaterial absorber structure show 90% of absorption at the lower resonating frequency and 92% of absorption at the higher resonating frequency under both transverse electric (TE) wave and transverse magnetic (TM) wave.

H. Li *et al.*, 2011 [16], proposed an ultrathin multiband metamaterial absorber working in the microwave frequency area. Firstly they formed a dual-band metamaterial absorber and then a multiband metamaterial absorber using a simple and efficient approach. For this, they presented two geometries in this paper. In the first design, two individual absorption peaks come out at 9.18 GHz and 12.35 GHz having a percentage absorption of 99.8% and 98.9%, respectively. Further, in the second drawing, three discrete absorption curves come out at 7.46 GHz, 10.43 GHz and 12.23 GHz having a percentage absorption of 99.1%, 94.8%, and 92.5%, respectively.

L. Li *et al.*, 2011 [17], proposed a different metamaterial absorber formed of a tetra-arrow resonator (TAR) geometry. The structure is designed in a way to obtain three absorption curves. The top layer is a metallic layer having a pattern of the tetra-arrow resonator and the bottom layer on the lower surface of the substrate is completely solid metal. Three diverse resonant modes of the propound absorber can be agitated by interacting with electromagnetic waves. Moreover, by optimizing the geometric parameters of the tetra-arrow resonator (TAR), a twice band, polarization-ineffective, compact and low profile metamaterial absorber structure whose absorptivity is almost perfect at two frequencies of

6.16 GHz and 7.9 GHz is obtained. The length and thickness of the substrate are 10.2mm and 2mm, respectively.

X. Shen *et al.*, 2011 [18], proposed design and measurement of a metamaterial-based microwave absorber which is resonating at three frequencies thus forming the triple-band absorber. The formed geometry is made of three closed ring resonators in the nested form. This proposed design is providing the absorption peaks at 4.06 GHz, 6.73 GHz, and 9.22 GHz with the absorptive percentage of 99%, 93%, and 95%, respectively. This structure is valid for diverse incident angles under both transverse electric (TE) and transverse magnetic (TM) polarizations. This geometry is printed on the dielectric substrate having length and thickness of 10mm and 0.78mm respectively.

H. T. Chattha *et al.*, 2011 [19], presented a planar inverted-F antenna with dual feed in which a single antenna can be used as a multiple input-multiple output (MIMO) antenna or diversity antenna and made suitable for wireless LAN (WLAN) applications. The proposed structure consists of one radiating plate and two feeding ports. Further, by amending the ground surface underneath the radiating plate, isolation is achieved. Thus the optimized size of the ground plane is taken as 100×40 mm^2. The results show that the ports provide the bandwidth of a minimum 50 MHz from 2.425 GHz to 2.475 GHz and cover the 2.45 GHz, WLAN band.

D. Kim *et al.*, 2011 [20], presented a twice band antenna forming a multiple inputs and multiple-output (MIMO) structure. The structure is comprised of two planar inverted-F antennas (PIFA) having a volume of $12 \times 10 \times 4$ mm^3 and two isolators which are placed in between the PIFA antennas to suppress the current flow between the antennas at the frequency bands 2.3 GHz and 3.4 GHz thus enhancing the isolation between the antennas. This whole structure is formed on the upper portion of the ground plane made of FR-4 substrate of thickness 1mm and having dimensions of 50×90 mm^2. This proposed structure provides the isolation value of -15 dB at 2.3 GHz and -22 dB at 3.4 GHz frequency band.

X. Y. Peng *et al.*, 2012 [21], proposed a seven absorption peak structure with an absorption rate of more than 90% while some peaks attain almost perfect absorptions with an absorption rate greater than 99%. In this structure, a dielectric layer is placed in between the two metallic layers thus forming a metal-insulator-metal waveguide. Further, electromagnetic waves propagate in the opposite direction within the substrate (dielectric layer) from contiguous gaps results in the standing waves within the waveguide. The thickness and length of the substrate are 3.4μm and 2μm, respectively.

Y. Liu *et al.*, 2012 [22], proposed a microwave-based metamaterial absorber having circular patches made of metal. The circular patch geometry is printed on the upper portion of the dielectric layer and a ground surface made of complete metal is printed on the lower side of the dielectric layer (substrate). Further, to maximize the frequency range of the projected structure, the number of circular patches are increased so that their resonating frequency peaks come closer to each other thus results in a broadband resonance. The proposed absorber provides full-width half maximum (FWHM) bandwidth of 2.8 GHz and a virtual full-width half maximum (FWHM) bandwidth of 25.3%. Moreover, the absorber operates at diverse incident angles under both transverse electric (TE) polarization and transverse magnetic (TM) polarization. The length of the substrate is taken as 40mm and the radius of the circular patch is taken as 3.5 mm.

L. Qiu *et al.*, 2012 [23], proposed an electromagnetic band-gap (EBG) structure along with a choke structure having mushroom-shaped geometry to provide isolation between the two large antenna elements. The electromagnetic band-gap (EBG) cells form a vertical structure to provide isolation. The proposed structure provides the isolation of about 30dB with a combination of electromagnetic band-gap (EBG) structure and the choke and about 22dB isolation only with the choke structure.

S. Bhattacharyya *et al.*, 2013 [24], proposed a metamaterial absorber geometry having an ELC resonator showing two different absorption curves at 5.04 GHz and 5.28 GHz with an absorption rate of 98.5% and 94.2%, respectively. Further, the proposed metamaterial absorber provides a full-width half maxima (FWHM) bandwidth of 0.42 GHz showing an 8.13% bandwidth. The proposed absorber geometry is considered under normal incidence angles along with oblique incident angles and FWHM bandwidth is maintained up to 40^{o} of incidence angle. The proposed absorber is also observed under diverse polarization angles up to 30^{o} of polarization angle, the absorber provides 7.4% bandwidth around the peak absorbance frequency.

H. M. Lee *et al.*, 2013 [25], proposed a single band metamaterial absorber. The projected design is made of an electric field coupled-LC (ELC) resonating geometry on the upper portion of the substrate and a metal ground (wire) on the lower portion of the substrate. Apart from the common metamaterial absorber configurations, a layer having a metal pattern is positioned analogous to the route in which incident wave propagates. The proposed metamaterial absorber showed an absorption curve at 10.1 GHz with the absorption percentage up to 86% regardless of the incident angle up to 60^{o}.

J. Tak *et al.*, 2013 [26], proposed a single band metamaterial based microwave absorber. This structure contains a connecting line with a resistor and two split-ring resonators (SRR) on the upper portion of the FR-4 dielectric substrate having dimensions of 30×35 mm^2 and the bottom side of the substrate contains the stripline which covers the area of 4.2×35 mm^2. The structure provides the peak

absorptivity of 97% at 2.45 GHz with the resistor value of 200 Ω and the half-maximum bandwidth of approximately 0.16 GHz. The peak absorptivity of the absorber at 2.45 GHz is maintained for the incident angle variation from 0^{o} to 60^{o}. Moreover, the transmission and reflectance at 2.45 GHz frequency band are obtained as 0.05 and 0.01 respectively**.**

T. M. Kollatou *et al.*, 2013 [27], proposed a systematic design of a polarization-independent metamaterial absorber with a confined design that operates in the microwave regime. A group of polarization-insensitive with compact size metamaterial absorber structures that attained a high absorption peak was introduced in this paper. The copper layers on the upper and lower part of the substrate were made of thickness 0.035mm, while the substrate was made of thickness 1mm. The peak value for the absorption for this proposed design is found to be 95.81% at 10.31 GHz. A large reduction in the absorption bandwidth for the incident angle greater than 60^{o} is observed. However, by the variation of the incident angles, the maximum absorption peaks remained unaffected.

S. Bhattacharyya *et al.*, 2013 [28], proposed a square-shaped closed ring resonating geometry having three absorption peaks along with polarization-insensitive behavior for airborne and radar signal absorption applications. The unit cell having various square loops were having its two absorption peaks in the C-band and one absorption peak in the X-band thus provided a tri-band response. Moreover, the absorber also provided a broader result with full-width half maxima (FWHM) bandwidth of 940 MHz having 9.43% bandwidth in the X-band. The absorber manifests the good absorption for a wide extent of incidence angles up to 60^{o}. The size of the structure was 18mm.

H. S. Singh *et al.*, 2013 [29], presented a multiple-input and multiple outputs (MIMO) twice band structure having low mutual linking between the antenna components. This antenna structure is operating in 2.4 GHz band ranging from 2.4 to 2.485 GHz and 5.5 GHz band ranging from 5.15 to 5.85 GHz. The presented design had very small volume i.e. $12 \times 9 \times 6$ mm^3 due to its folded structure and slots on patch. Further, a folded shorting strip was allied between the individual antenna element and the ground surface to enhance the port to port isolation. The structure shows the isolation value less than −28 dB over the lesser value frequency band i.e. 2.4 - 2.485 GHz and better than -26dB over the higher frequency band i.e. 5.15 - 5.85 GHz.

H. S. Singh *et al.*, 2013 [30], proposed multiple inputs and multiple output antenna having a spiral-shaped structure that covers the frequency bands LTE700 (ranging from 777-787), GPS-L1 (ranging from 1565-1595), and WLAN (ranging from 2400-2480). The defected ground structure (DGS) having a double rectangular ring-shaped slot was formed to attain the separation between the ports. Thus the remoteness value lower than -20dB for LTE, -21dB for GPS-L1 and -18 dB for the WLAN band between the ports is achieved respectively. The proposed structure showed good diversity

performance with diversity gain of about 10 for all the three bands and also envelope correlation coefficient (ECC) is having a value less than 0.05.

H. S. Singh *et al.*, 2013 [31], presented a planar inverted-F structure antenna with compact size providing triple-band resonance in LTE band having range from 765 MHz to 787 MHz, PCS1900 band having range from 1850 MHz to 1920 MHz and WiMAX having range from 3.05 MHz to 3.65 GHz with -6dB return loss. The presented structure was formed of an L-shaped slot along with an interdigitated strip which is also folded on the back portion of the substrate providing the remoteness between the ports lesser than -10dB for all the three working bands. The proposed geometry is formed on the FR-4 dielectric substrate and the ground surface is having dimensions $50 \times 100 \times 0.8$ mm^3. Further, the antennas are mounted at a height of 4.8mm from the ground surface and these antenna elements are having the dimensions $7 \times 9.75 \times 0.8$ mm^3.

R. Puri *et al.*, 2014 [32], proposed a structure which provides absorption of the electromagnetic wave at a resonance frequency of 10.5 GHz. Absorption of 74% was achieved at 10.5 GHz and reflection was reduced to 20% at the resonance frequency of 10.5 GHz. Silver was used for designing the cut wire which affects the transmission and thus led to the transmission of only 6%. The material used for dielectric was FR-4 with a height of 12mm and thickness of 0.5mm. Copper was used as an ERR material having a thickness of 0.1 mm. The material used for wire was silver with a thickness of 0.1 mm.

S. Jamilan *et al.*, 2014 [33], presented a design of metamaterial absorber which showed two absorption peaks in the microwave area. The projected metamaterial absorber was having a metallic gammadion shaped structure made of metal printed on the upper portion of the dielectric spacer and a complete layer of metal on the backside of the dielectric spacer. The proposed structure showed two absorption curves at 5.6 GHz and 6 GHz having an absorption level of 97% and 99%, respectively. The top layer of the design had a gammadion-shaped structure and the bottom layer had a complete ground plate. The spacer of the absorber structure was the FR-4 with 1.5mm thickness and length 20mm. Each of the metallic layers was made of copper with 0.02mm thickness.

S. Bhattacharyya *et al.*, 2014 [34], presented a low profile ultrathin metamaterial based microwave absorber contained patches having L-shaped geometry made of copper, located at diagonal positions at the top portion. The presented structure showed broader results in C-band. The bandwidth of the absorptive curve ranging from 4.6 to 7.2 GHz with more than 90% absorptivity at 2.6 GHz frequency was provided. The proposed structure has been observed under oblique incidence, both for transverse electric and transverse magnetic polarizations providing a wider absorption response up to 45º incidence angles in both cases. The rear portion of the structure was completely made of copper and

divided by the FR-4 substrate having thickness 3.2mm from its front surface. Further, the absorption bandwidth of 2.6 GHz between 4.6 GHz and 7.2 GHz frequency range has been observed with more than 90% absorptivity along with the absorption percentage of 99.8% at 4.90 GHz and 99.9% at 6.56 GHz.

R. Puri *et al.*, 2014 [35], proposed a metamaterial-based resonant absorber. The proposed structure provides the absorption of 74% at 10.5 GHz resonant frequency and the reflection was reduced to 20% at this resonant frequency. The structure was printed on the dielectric substrate made of FR-4 material height 12mm, width 4.2mm and thickness 0.5mm. Moreover, the material used for the resonating structure was copper of thickness 0.1mm and the material used for the cut wire was silver of thickness 0.1mm which effected the transmission of the electromagnetic wave and transmission was only 6%.

S. Bhattacharyya *et al.*, 2014 [36], proposed a low profile ultrathin geometry of three concentric closed ring resonators (CRR) having polarization-independent nature. Different geometrical parameters such as radii of the closed rings, width of the closed rings as well as unit cell size was optimized as a result of which absorption took place at three different frequencies with different absorption percentages i.e. at 5.50 GHz with 94.1%, at 9.52 GHz with 99.6% and 13.80 GHz with 99.4%. The length of the structure was taken 10mm and the thickness of the substrate was taken 1mm.

O. Ayop *et al.*, 2014 [37], designed a metamaterial-based microwave absorber unit cell of dimensions 9 mm × 9 mm for dual-band applications. The structure was having two resonating rings which were functioning at 9 GHz and 11 GHz. The proposed geometry was having a circular ring made of copper metal and this geometry was formed on the top portion of the FR-4 substrate. The bottom portion of the substrate consisted of complete copper which is termed as the ground surface. The two band metamaterial absorber structure is made to work at diverse incident angles for both transverse electric (TE) and transverse magnetic (TM) waves. The shape of the design was symmetrical in nature, therefore it was polarization-insensitive in nature. Metamaterial absorber had a full-width half maximum (FWHM) between 4% and 5%. The average radius of the copper rings was 2.975 mm and 2.51 mm whereas the width of the rings was 0.25 mm and 0.28 mm respectively.

B. Y. Wang *et al.*, 2014 [38], formed a design of compact, ultrathin double-layer metamaterial absorber structure providing a broadband response. The structure made was simple along with the polarization-insensitive nature. The proposed broadband absorber provided the absorption percentage greater than 90% between the frequency range of 8.85 GHz and 14.17 GHz. Further, the proposed broadband absorber was having a full-width half maximum (FWHM) absorption bandwidth of 6.77

GHz along with full width half maximum (FWHM) absorption bandwidth of 57.3%. The proposed absorber was having a thickness of 1.6 mm.

T. M. Kollatou *et al.*, 2014 [39], presented an ultra-thin metamaterial based microwave absorber with a single band, twice band and then further extended to the triple band. The top surface of the dielectric substrate consisted of the electric ring resonator and the bottom surface of the dielectric substrate consisted of a pair of crossed wires. Moreover, multiple unit cells of the same structure were placed adjacent to each other to get dual-band and further triple-band at different resonating frequencies. The length and thickness of the dielectric substrate were taken 5.5mm and 1mm respectively. The absorption peak appeared at a frequency of 11.03 GHz with an absorption percentage of 81.61% for the single-band structure, two absorption peaks occur at 11.84 GHz and 14.70 GHz with absorption an rate of 91.79% and 98.74% respectively for dual-band structure. Further, three absorption peaks occur at 9.78 GHz, 97.43% and 11.78 GHz with peak absorptivity of 98.89%, 97.43%, and 98.54% respectively for triple-band structure.

S. Ghosh *et al.*, 2014 [40], discussed a compact polarization-independent metamaterial absorber. The formed design which was printed on the FR-4 dielectric substrate of dimensions $5 \times 5 \times 1$ mm^3 has a swastika-like structure. This structure provides the peak absorption at 10.10 GHz with an absorptivity of 99.64%. The proposed absorber provided maximum absorption for diverse polarization angles and also for diverse incident angles up to 60^o due to its symmetric structure. Further, the design was extended to 2×2 array having diagonally identical elements. This structure was optimized to reduce the distance between the absorption peaks and provide a broader response with a half maximum of 0.68 GHz (10.04–10.72 GHz). The bandwidth improved structure is also polarization-insensitive and also maintains its enhancement property up to 60^o of incident angle.

H. S. Singh *et al.*, 2014 [41], proposed a multi-input multi-output ultra-wideband (UWB) planar inverted-F antenna (PIFA). This design consisted of a top-loaded capacitive plate of dimensions 20×10 mm^2 and a rectangular monopole as a feed plate of dimensions 14×6.75 mm^2 forming the T-shaped structure. This T-shaped structure was grounded through the shorting wall. The design was formed on the FR-4 dielectric substrate acting as a PCB for the whole structure having 4.4 dielectric constant 0.018 loss tangent. The proposed structure covered the wide frequency range from 3.0 GHz to 10.8 GHz giving percentage impedance bandwidth of 113% and provided the isolation less than -15 dB between the antenna elements.

Y. J. Yoo *et al.*, 2015 [42], proposed a tri-band metamaterial perfect absorber having a cut wire bar pattern. The optimized structure has dimensions of 15mm × 16mm in two planes i.e. x plane and y plane. The thickness considered of the dielectric substrate was 2.4mm. The absorption peak was also studied at different rotation angles by turning the cut wire bar from 0^o to 90^o. It was observed that the absorption of two absorptivity curves was reduced as the cut-wire bars were rotated from 0^o to 90^o along with the occurrence of new absorption curves. Further, only a single absorption a peak existed at 10.78 GHz with peak absorptivity of 81% at a rotation angle of 90^o. Furthermore, three absorption curves at 5.68 GHz, 11.05 GHz and 16.63 GHz with the peak absorptivity of 84.1%, 93%, and 61.1% occur at the rotation angle of 45^o.

H. Zhai *et al.*, 2015 [43], proposed a compact metamaterial absorber along with polarization insensitivity property having three absorption peaks. The structure consisted of a metallic background plane. The thickness and length of the FR-4 dielectric substrate are 1mm and 11mm respectively. The structure showed the polarization-insensitive characteristic over the different angles for both transverse electric (TE) and transverse magnetic (TM) waves. This gave triple absorption curves at 3.25 GHz, 9.45 GHz, and 10.90 GHz with the absorption levels of over 90%. Further, while changing the incident angle from 0^o to 60^o, the three absorption curves remained at the same frequencies along with the good absorptivity peaks. Also, the proposed absorber design was polarization-insensitive in nature as it was providing the same absorption curves at the three resonating frequencies i.e. 3.25 GHz, 9.45 GHz, and 10.90 GHz.

S. Bhattacharyya *et al.*, 2015 [44], proposed a polarization-independent enhanced bandwidth metamaterial absorber structure. The projected structure consisted of two layers of the dielectric substrate. Through the parametric optimization process, a design was formed on the top portion of the two dielectric layers and the absorption curves with enhanced bandwidth were obtained in the C-band and X-band. The proposed design was polarization-insensitive in nature as this bandwidth enhanced the characteristic of the dual-band structure remained the same for any polarization angle under normal incidence angle. The presented absorber design provided the absorptivity curve at eight frequency bands i.e. 6.56 GHz, 6.76 GHz, 7.08 GHz, 8.60 GHz, 9.20 GHz, 9.48 GHz, 9.86 GHz and 10.20 GHz having the absorption of about 99.3%, 94%, 90.9%, 99.8%, 82.5%, 83.3%, 93.4% and 61.6 %, respectively. Two separate FR-4 substrates of length 20mm and thickness 1.6mm were used in the fabrication of the structure.

D. Chaurasiya1 *et al.*, 2015 [45], presented a low profile three-band metamaterial absorber lying in C-band. The geometry of the proposed metamaterial absorber consisted of three concentric rings made of metal on the upper portion of the dielectric substrate having length 24mm and a complete metal ground was made on the lower portion of the dielectric substrate. The proposed metamaterial absorber

does not vary with the polarization angles thus making it polarization-insensitive in nature as the structure exhibited the four-fold symmetry. The triple band absorber provided the peak absorptivities of about 96.84%, 99.85% and 96.99% at 4.32 GHz, 6.05 GHz, and 7.30 GHz, respectively.

D. Sood *et al.*, 2015 [46], proposed a design of low profile metamaterial based microwave absorber with wideband characteristics. An array of the projected absorber design was made and observed under different polarization angles. The geometry formed of metal on the top part of the dielectric substrate consisted of four circular slots which were made symmetrically concerning the center of the proposed metamaterial absorber unit cell. Circular slots geometry was responsible for the resonance peak at a lower frequency band while the hexagonal geometry patch was liable for the resonance peak at a higher frequency band. The proposed wideband absorber design provided the absorptivity greater than 90% from the frequency range of 5.27 GHz to 6.57 GHz. The thickness of the substrate made was 1.6mm.

H. S. Singh *et al.*, 2015 [47], presented a multi-input multi-output (MIMO) triple-band antenna. The projected structure consisted of two planar inverted-F antennas (PIFA) on the upper side of the circuit board made of FR-4 material of dimensions $100 \times 60 \times 0.8$ mm^3 having folded patch structure along with two upright parasitic strips and having a volume of $9 \times 8.8 \times 5.4$ mm^3. This structure provided the isolation less than -15 dB for 2.45 GHz band from the frequency range of 2.4 GHz to 2.485 GHz and 5.5 GHz band from the frequency range of 5GHz to 5.8 GHz, and -10 dB for 3.4 GHz band from the frequency range of 3 GHz to 3.45 GHz without using the folded shorting pin. Further, to improve the isolation between the ports, two folded shorting pins are attached in between each antenna component and a ground surface and then the remoteness achieved for all the frequency bands is less than -16dB. Thus, the improvement in isolation was 13 dB at 2.45 GHz frequency band, 5 dB at 3.4 GHz frequency band, and 12 dB at 5.5 GHz frequency band.

A. Agrawal *et al.*, 2016 [48], projected a polarization-independent metamaterial absorber lying in C-band, X-band and Ku-band frequency ranges having concentric uninterrupted ring resonating geometry. The concentric rings were made in four quadrants having different radii and width on the FR-4 dielectric substrate of length 18mm. The proposed absorber geometry consisted of four subcells in which sub-cells 1 and 4 are identical and in a similar way sub-cells 2 and 3 are identical. The identical rings are placed at diagonal positions. The proposed absorber provided four absorption peaks with peak absorptivity of 98%, 98%, 96% and 92% at frequencies 7.102 GHz, 9.104 GHz, 12.558 GHz, and 13.097 GHz, respectively. Further, it is also noted that two end peaks provide a broader response as they were very close to each other.

S. Bhattacharyya *et al.*, 2016 [49], presented a wide absorption bandwidth structure for defense applications. The structure consisted of a geometry of a single circular split ring made of metal which is formed on the top portion of the dielectric substrate having a thickness of 3.2mm. Four distinct absorption peaks have been achieved at 6.46 GHz with the absorptivity percentage of 99.8%, at 10.24 GHz with the absorptivity percentage of 99.9%, at 15.26 GHz with the absorptivity percentage of 99.6% and 16.66 GHz with the absorptivity percentage of 92.2%. Copper patches had been used as metals in the design and are of 0.035mm thickness.

S. Ramya *et al.*, 2016 [50], proposed a twice band metamaterial absorber at C-band and X-band which is polarization insensitive in nature which can be used for radar applications. The proposed absorber geometry consisted of a circular resonator surrounded in the square resonator. The FR-4 dielectric substrate of length 10mm and thickness 1mm with the metallic grounded bottom is used. The proposed design provided the absorption curve at 5.5 GHz and 8.9 GHz with a peak absorptivity percentage of 99.8% and 99.97%, respectively. Further, the proposed design is also polarization-insensitive in behavior.

A. M. Montaser *et al.*, 2016 [51], proposed a tri-band metamaterial absorber for different applications. The proposed design resonated at triple different frequencies i.e. 2.8 GHz, 4.1 GHz and 5.8 GHz having absorption peaks of around 99%, 99%, and 89% respectively. The geometry of the proposed design consisted of a hexagonal resonator along with a cross mark at the center and the cross mark was enclosed within split-ring resonators. This whole geometry was made of metal and printed on a dielectric substrate. Due to the rotational evenness of the geometry from all the sides, the magnitude and frequency of the absorption curve do not vary with the polarization angle from 0^o to 90^o thus making it polarization-insensitive in nature.

M. Agarwal *et al.*, 2016 [52], presented a planar inverted-F antenna (PIFA) which uses an array of the metamaterial unit cell to provide isolation between the antenna elements of dimensions 12×5 mm^2. These antenna elements are at a height of 5.8 mm from the ground surface of dimensions 100×40 mm^2. The metamaterial dual-band microwave absorber which is used as an isolator in this paper is of 4×2 arrays and having a size of $13 \times 12 \times 0.8$ mm^3. The isolation between the antenna elements increases from 22.5 dB to 33 dB for band 1 i.e. 5.15 GHz to 5.35 GHz and band 2 i.e. 5.725 GHz to 5.825 GHz respectively.

K. P. Kaur *et al.*, 2017 [53], designed a two-band metamaterial based microwave absorber having polarization-insensitive nature. The geometry of the proposed absorber structure consisted of two concentric closed ring resonator design thus forming octagonal rings shaped structure providing absorption at two frequencies that are 2.09 GHz and 2.54 GHz. Moreover, the absorption peaks

having peak absorptivity of 99.88% and 98.67% at the resonating frequencies 2.09 GHz and 2.54 GHz respectively are obtained with minimum reflection coefficients of −29.15 dB and −18.76 dB. This structure is embedded in the FR-4 dielectric substrate of length 27.4mm and thickness 2.4mm.

Y. Z. Cheng *et al.*, 2017 [54], proposed an ultra-thin metamaterial absorber having polarization-insensitive behavior. The absorber design consisted of a single circular sector resonator geometry and showed multi resonant peaks. They firstly presented a tri-band metamaterial absorber at frequency 3.35 GHz having peak absorptive percentage of 98.8%, at frequency 8.65 GHz having peak absorptive percentage of 99.7% and at frequency 12.44 GHz having peak absorptive percentage of 98.3% with the help of single circular sector resonant geometry. The proposed metamaterial was 0.8 mm thick and the length of the substrate was taken 20mm. Further, quad-band and pentaband metamaterial absorbers are proposed by selecting the suitable geometric parameters of the absorber unit cell. Moreover, it was shown that the projected absorber design is polarization insensitive in nature as the absorptivity curve does not varied with the variation of polarization angle from 0^o to 90^o.

Y. Z. Cheng *et al.*, 2017 [55], proposed an ultrathin perfect metamaterial absorber (PMMA) in terahertz range having six bands with an average absorption rate of up to 95% at these six resonant frequencies. The design consisted of cross-cave shaped geometry located over a ground plane. A ground plane made of copper was separated by a thin lossy Gallium Arsenide (GaAs) dielectric film. The length of the substrate was chosen as 75μm and the thickness of the substrate was 3.8μm. The copper film was having a thickness of 0.6μm. The absorption peak occurred at resonant frequencies of 1.13 THz, 1.56 THz, 1.77 THz, 2.18 THz, 2.85 THz, and 3.14 THz with absorptivity of 90.5%, 94.4%, 98.7%, 96.2%, 95.4%, and 95.2%, respectively.

S. K. Sharma, 2017 [56], designed a low profile dual-band metamaterial absorber which has been utilized for the X-band and Ku-band applications. The projected metamaterial absorber consisted of cross-spanner shaped geometry enclosed within a square patch. This structure was fixed on the top of the dielectric substrate which is backed with the copper metal of 8mm length and 0.25mm thickness and thickness of the copper metal was 0.017mm. The designed absorber has symmetric shaped structure and therefore it was polarization-insensitive in nature.

X. Yu *et al.*, 2017 [57], designed a multiband metamaterial absorber using a CST microwave studio. The proposed metamaterial absorber design provided multiple absorption curves at 4.64 GHz having peak absorption percentage of 99.6%, 8.67 GHz having peak absorption percentage of 99.8%, 13.93 GHz having peak absorption percentage of 99.9% and 18.53 GHz having peak absorption percentage of 93.5%. The proposed metamaterial based microwave absorber was having a thickness of just 3.3%, 6.3%, 10.0% and 13.3% of its operational wavelength respectively. The length of the resonator was

taken 10.8mm. The dielectric substrate of the projected absorber was having a thickness of 0.72mm and the copper metal was having a thickness of 0.035mm.

N. Mishra *et al.*, 2017 [58], designed a low profile tri-band metamaterial absorber for different microwave frequency applications. The projected structure was also polarization-insensitive in nature as the geometry of the absorber was having symmetricity. This design consists of two resonating structures and both the resonating structures are formed on the upper portion of the FR-4 epoxy glass substrate having a thickness of 0.8mm and length 8mm. One structure is liable for the first absorption peak and the second structure is liable for the other two absorption peaks. The proposed structure showed three absorption curves at 4.19 GHz, 9.34 GHz and 11.48 GHz having absorptive percentages of 99.67%, 99.48%, and 99.42% along with the FWHM bandwidth of 170 MHz from 4.11 GHz to 4.28 GHz, 350 MHz from 9.17 GHz to 9.52 GHz and 480 MHz from 11.24 GHz to 11.72 GHz, respectively.

V. A. L. Mol *et al.*, 2017 [59], proposed a low profile ultra-thin metamaterial absorber with better bandwidth along with polarization-insensitive behavior. The proposed design absorptivity curves attributes showed good absorption rates even with the variation of the incidence angle up to 40°. This absorber design provides good angular stability up to 60°. The absorber geometry was formed on the upper portion of the FR-4 dielectric substrate having a thickness of 1.6mm. Moreover, the design showed two absorption curves at 5.25 GHz and 5.37 GHz with a maximum absorptive percentage of 99.79% and 97.75%, respectively. Further, to broaden the resonance response, a 2 × 2 array of the structure is formed in which diagonal cells are identical in size. This 2 × 2 array helped to improve the bandwidth up to 0.574 GHz. The absorption curve was noted at 5.06 with a peak absorptive percentage of 92.52%, 5.245 with peak absorptive percentage of 99.45% and 5.32 GHz with peak absorptive percentage 99.77%. The length of the substrate was chosen 20mm for a simple structure and 40mm for bandwidth enhanced structure. Moreover, the thickness of the substrate was 1.6mm.

S. R. Thummaluru *et al.*, 2017 [60], presented a design and analysis of the metamaterial based microwave absorber having triple-band resonance. The proposed design was taken as a mixture of two absorber structures named as absorber-I and absorber-II. Absorber-I and absorber-II were separately liable for the resonant frequency at 4.2 GHz and 7 GHz respectively and mutual linking between both the absorbers i.e. absorber-I and absorber-II resulted in the absorption at one more frequency i.e. 7.4 GHz. Thus, the proposed structure which is the mixture of absorber-I and absorber-II resulted in the absorption of 91%, 98.9% and 99.5% at the resonant frequencies of 4.2 GHz, 7 GHz, and 7.4 GHz, respectively. Moreover, the proposed structure does not varied with the change in the polarization angle thus making it polarization-insensitive in behavior. The proposed design and the ground portion

are separated by the dielectric substrate made of FR-4 material having a length of 28.2mm and thickness of 1.6mm.

J. Wang *et al.*, 2018 [61], projected a polarization-independent metamaterial based microwave absorber. The projected design was made of a set of wires engraved on an ultrathin Teflon dielectric substrate. The presented absorber patch was imprinted on the Teflon dielectric substrate having a length of 11mm. Further, for the transverse magnetic (TM) polarization, a single band absorption curve at 6.64 GHz having absorptivity of 99.8% was achieved and for the transverse electric (TE) polarization, pentaband absorption curves at 11.68 GHz, 13.58 GHz, 15.48 GHz, 17.38 GHz, and 19.28 GHz frequency bands having absorptivity of more than 99% was achieved.

S. Fan *et al.*, 2018 [62], presented a metamaterial-based microwave absorber showing absorption curve at 442MHz with peak absorptivity of 99.73%. The structure is made of a metallic ground surface. The proposed absorber geometry and the ground portion are divided by a dielectric substrate and air. The thickness of the top copper geometry and the bottom ground surface was taken as 0.035mm. The ground portion and the dielectric substrate were separated by air portion having a thickness of 8.6mm. The length and thickness of the dielectric substrate were taken as 10mm and 1mm respectively. The unit cell of the projected absorber was simulated using CST Microwave Studio. Further, it was noted that the full width half maximum (FWHM) of the proposed absorber was 5.6% ranging from 430 MHz to 455 MHz.

R. Sekar *et al.*, 2018 [63], proposed an ultrathin wideband metamaterial absorber having circular and rectangular split rings of dimensions $8 \times 8 \times 1$ mm^3. The proposed design provided the wideband response of 3.84 GHz with a 90% absorption curve from 12.80 GHz to 16.64 GHz and two resonance peaks were noted at 13.2 GHz and 16.5 GHz. The full width half maximum (FWHM) of the proposed design was noted from 12.09 GHz to 17 57 GHz of 5.48 GHz. However, the proposed wideband metamaterial absorber was polarization-sensitive in nature. Moreover, the wideband absorption was attained only for definite normal and oblique angles of incidence, with decreased absorptivity curve.

R. Asgharian *et al.*, 2018 [64], discussed a triple-band metamaterial absorber which was having a T-shaped and square-liked ring resonator. The proposed structure provided the absorption peaks of 95%, 97% and 99% at 5.8 GHz, 9.52 GHz, and 11.97 GHz, respectively. Moreover, the projected absorber provided wide-angle stability under both transverse electric (TE) and transverse magnetic (TM) polarizations. The proposed design was printed on the FR-4 dielectric substrate having thickness and length of 1mm and 9.3mm respectively.

2.2 RESEARCH GAPS

Based on the above literature survey, the following gaps are identified:

a. The size of the absorber is still a scope of research as modern technology going toward miniaturization. Therefore, compact/small microwave absorber can be addressed to meet the expectation. Some of the ultrathin microwave absorbers are presented by researchers but super ultrathin along with compact structure is another scope of research.

b. The polarization insensitive along with compact structures with almost perfect absorption should be addressed to make them more effective for practical applications.

c. The wideband microwave absorber which includes most of the microwave frequency bands in a single absorber is highly demanding.

d. The wideband absorber along with compact structure is one of the challenging researches in the current scenario. Therefore, a compact wideband metamaterial based microwave absorber can be addressed.

e. PIFA structure with compact size and improved isolation is another scope of research.

2.3 OBJECTIVES OF THE THESIS

a. Design and simulation study of ultra-compact polarization-independent dual-band metamaterial absorber resonating at 5.65 GHz and 10.91 GHz. Further, a parametric study on the proposed absorber design along with fabrication and testing proposed metamaterial absorber.

b. Design and analysis of a compact ultrathin polarization- and incident angle-independent triple-band metamaterial absorber with peak absorption at 3.4GHz, 9.6GHz and 13 GHz. Fabrication and testing proposed metamaterial absorber.

c. A compact metamaterial-based wideband absorber with wideband absorption of 9 GHz Fabrication and testing proposed wideband metamaterial absorber.

d. Isolation improvement of the MIMO PIFA using metamaterial absorber array at 5.65GHz frequency. Fabrication and testing proposed PIFA design.

CHAPTER 3

SIMULATION STUDY OF ULTRA COMPACT POLARIZATION INDEPENDENT DUAL-BAND METAMATERIAL ABSORBER

3.1 INTRODUCTION

Several metamaterial absorbers have been developed and studied which are made of different attributes, such as one band, two-band, three-band, and four-band. Numerous works have been done on a double band metamaterial based microwave absorber. However, the need for an absorber nearly perfect absorptivity (close to unity), ultra-thin, low profile and the low-cost substrate is still scope of study which needs to be explored.

In our design, a compact ultrathin metamaterial absorber is projected for C-band and X-band applications. The projected structure provides 98.8% absorption at 5.65 GHz and 99.5% absorption at 10.91 GHz for transverse electric (TE) mode and transverse magnetic (TM) mode. The design is also studied for transverse electric (TE) mode and transverse magnetic (TM) mode at diverse incident angles. Moreover, due to even geometry, the proposed unit cell provides polarization insensitivity.

3.2 CONFIGURATION AND DESIGN OF DUAL-BAND ABSORBER

3.2.1 Absorber configuration

The proposed absorber is intended on the low-cost FR4 substrate of dielectric constant 4.4 and loss tangent (tan δ) =0.018. The absorber is a sandwich of two layers made of metal divided by a dielectric substrate of thickness 0.8mm. The configuration of the designed absorber is shown in Figure 3.1. The top layer consists of the metallic resonating structure while the underneath layer is completely laminated with copper. The proposed absorber consists of two resonating geometries i.e. swastika-shaped structure enclosed within a square ring. The thickness of all copper geometry (patch and ground) is 0.035mm. The optimized shape parameters are scheduled in Table 3.1. The numerical simulation of the proposed absorber is accomplished using the finite integration technique based computer simulation microwave studio (CST MWS) by applying Floquet periodic boundary conditions. However, the absorptivity $A(\omega)$ of the metamaterial absorber is calculated by using the formula as given in the appendix.

Table 3.1 Design Parameters of Absorber

Parameters	Size (mm)	Parameters	Size (mm)
A	6	w_2	0.25
B	5.6	l_1	1.9
w_1	0.1	l_2	3
D	1		

3.2.2 Design of absorber

The design progress of the projected absorber is presented in Figure 3.2. There are three steps are considered to obtain the fine configuration of the absorber as shown in Figure 3.2(a) and absorptivity curve relative to each configuration is shown in Figure 3.2(b). From, Figure 3.2(b), it is noted that the swastika-shaped geometry is mainly responsible for higher resonance centered at 10.91 GHz while the square-shaped ring is resonating at 5.65 GHz. Finally, the combined structure of swastika-shaped and square ring-shaped provides dual absorbance at 5.65 GHz and 10.91 GHz. The resonating behavior of the swastika-shaped and square ring shape geometries at 10.91GHz and 5.65 GHz are also confirmed by surface current distribution as presented in Figure 3.3. It is perceived that at 5.65 GHz, the maximum current concentrated at the outer ring while at 10.91 GHz, the maximum current concentrated at the swastika-shaped structure. Therefore, two independent structures provide the dual absorbance nature of the proposed structure. Moreover, the mutual coupling between these two structures provides better impedance matching which results in enhancement of the absorbance with the highest absorptivity of 98.8% and 99.5% at 5.65 GHz and 10.91 GHz, respectively.

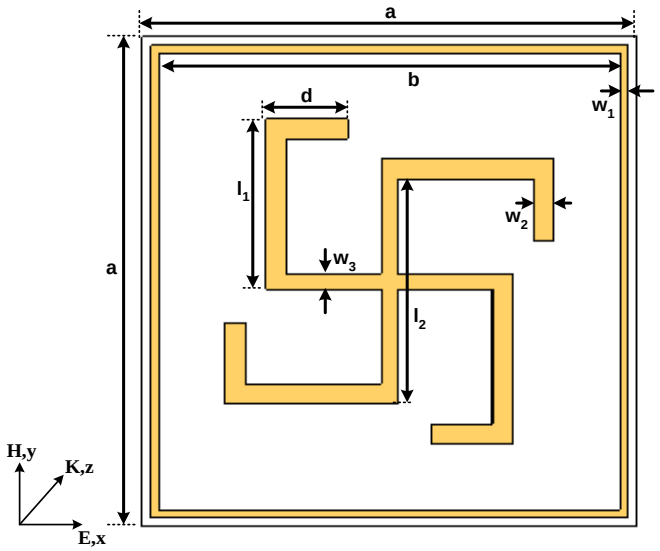

Figure 3.1 Detailed dimensions of the proposed absorber

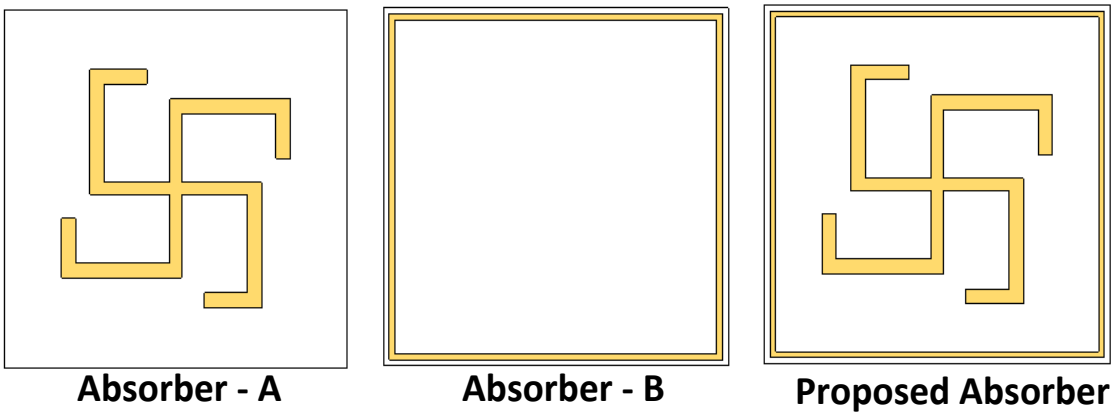

(a)

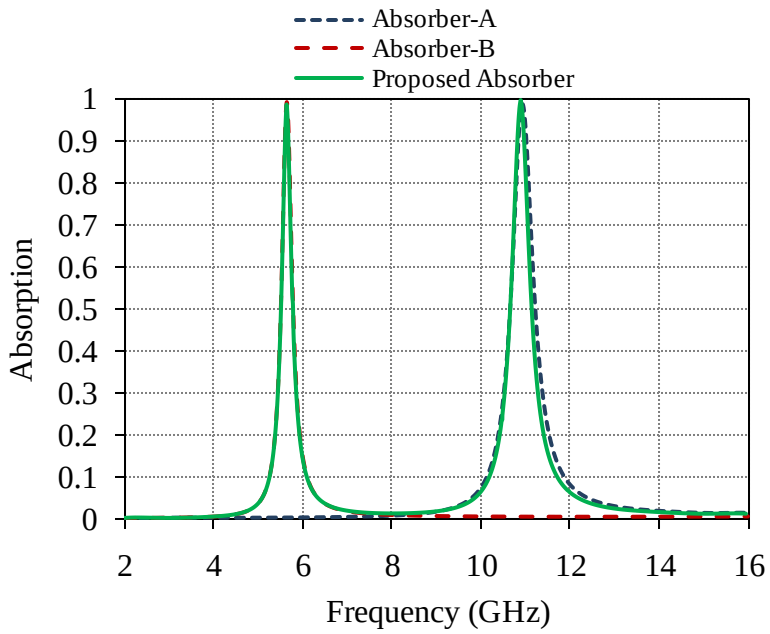

(b)

Figure 3.2 (a) Evolution of the proposed absorber, (b) Variation of absorptivity due to various configurations

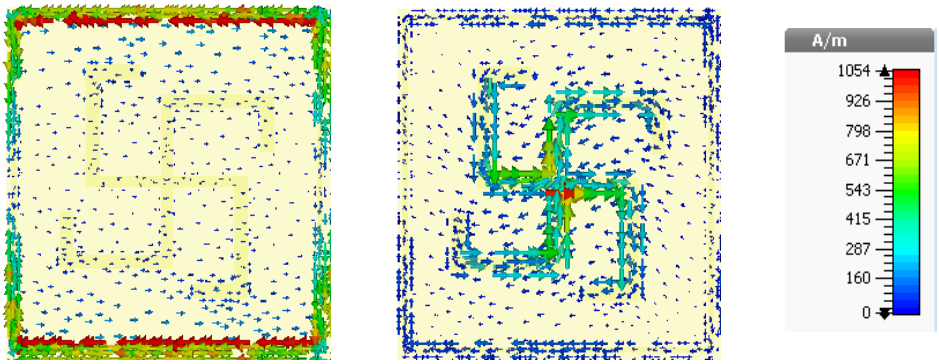

Figure 3.3 Surface current distribution at 5.65 GHz and 10.91 GHz

3.3 RESULTS AND DISCUSSIONS

All the simulations have been accomplished using CST MWS. Normal angle and oblique angles of incidence are measured to study the polarization sensitivity of the design. The analysis is carried out by varying the polarization angle keeping the incident angle constant as shown in Figure 3.4. It is observed that the absorption curves are overlapped each other when the polarization angle varies from 0^{o} to 60^{o}. Therefore, no variation at different polarization angles making it polarization-insensitive in nature this is mainly due to the fourfold symmetric structure. Furthermore, it is also observed that the proposed absorber provides the same absorptivity for both modes i.e. transverse electric (TE) mode and transverse magnetic (TM) as shown in Figure 3.5.

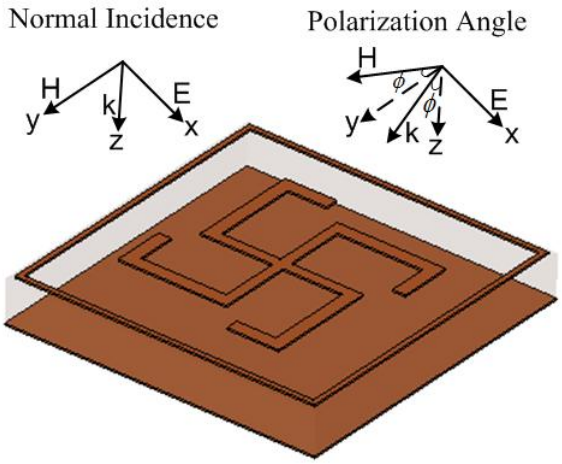

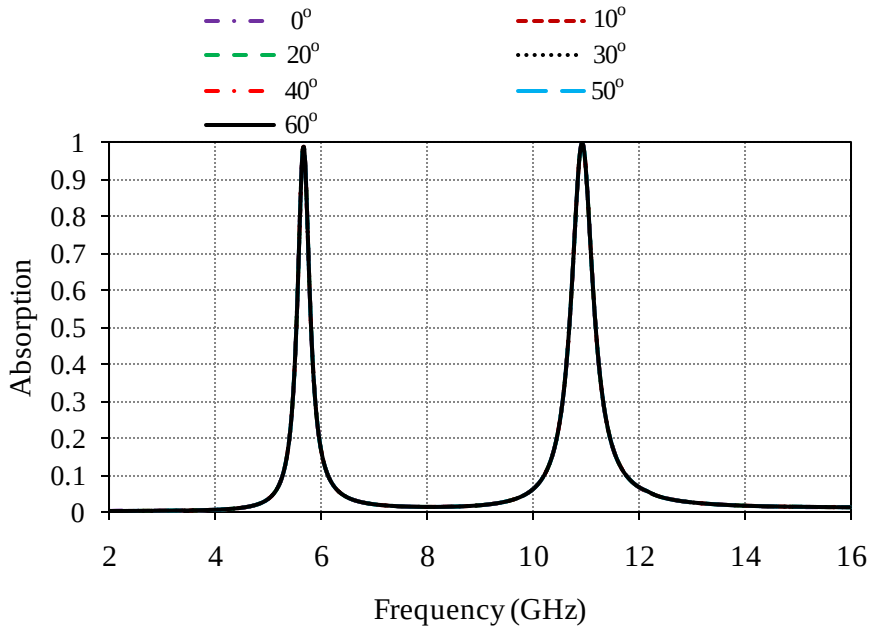

Figure 3.4 Variation of absorptivity with polarization angle (ϕ)

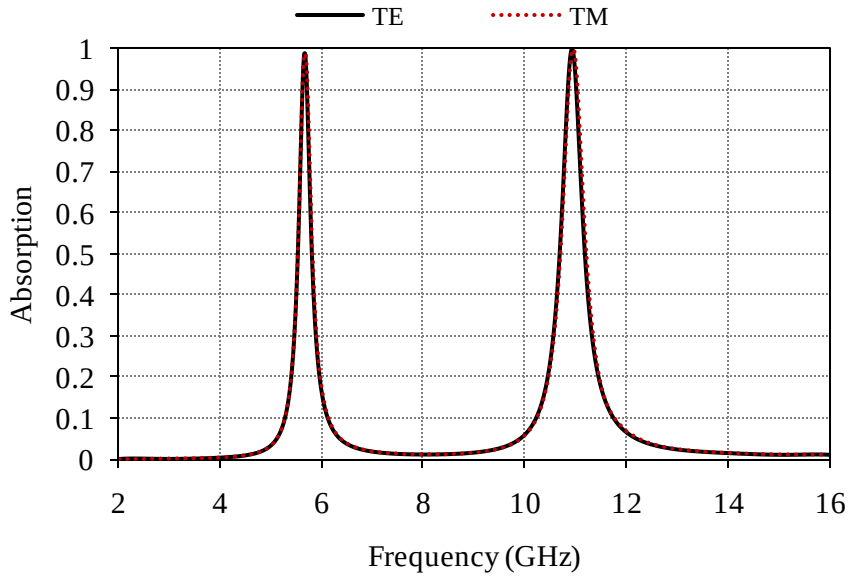

Figure 3.5 TE and TM absorptivity curve

Further, the variation of absorption with different incident angles is presented in Figure 3.6. Figure 3.6(a) shows the variation of absorptivity by changing the direction of the magnetic field and wave vector by an angle θ and keeping the direction of the electric field fixed. Figure 3.6(b) shows the variation of absorptivity by changing the direction of the electric field and wave vector by an angle θ and maintaining the direction of the magnetic field fixed. It is interestingly noticed that the slight variation in the absorption peaks along with small side peaks are occurred as when we are changing the incident angle from normal to oblique. The same phenomenon happened in TE and TM polarized incident angle variation.

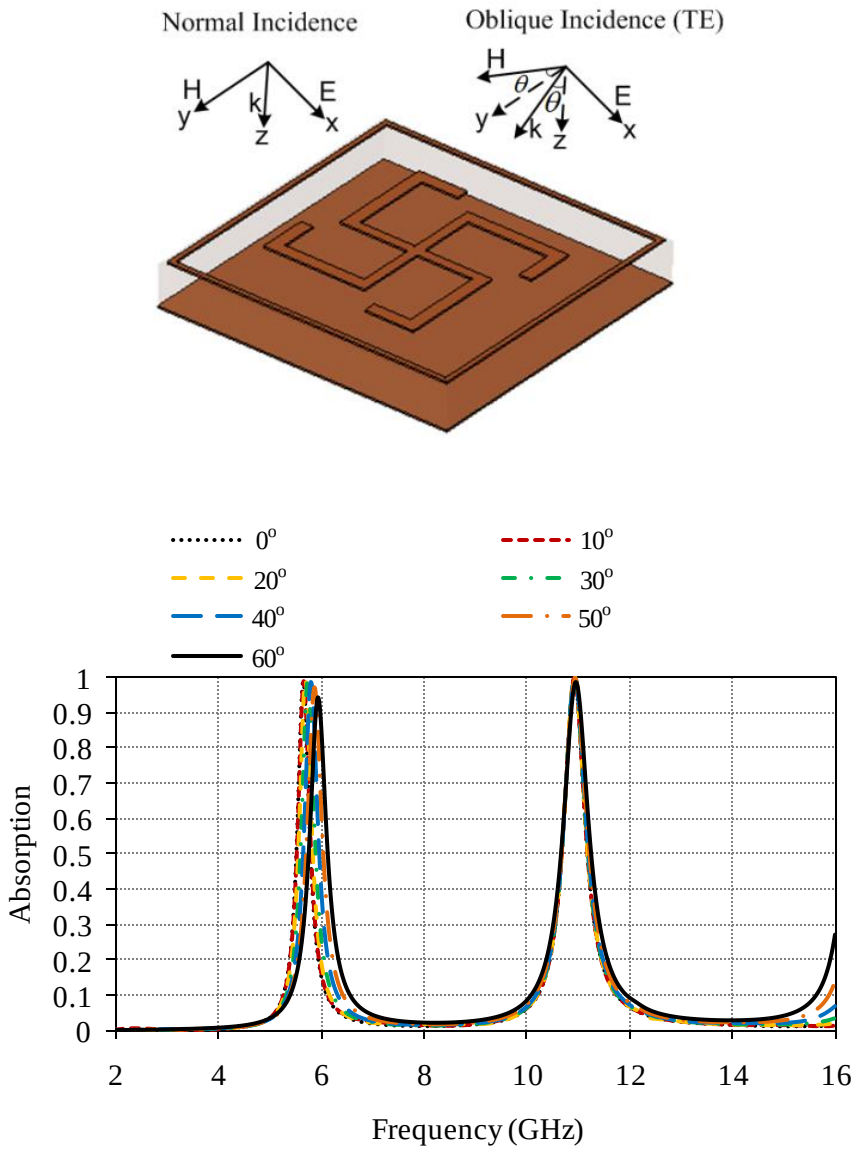
Normal Incidence
Oblique Incidence (TE)
H
E
k
y
x
z
θ
0°
10°
20°
30°
40°
50°
60°
Absorption
1
0.9
0.8
0.7
0.6
0.5
0.4
0.3
0.2
0.1
0
2
4
6
8
10
12
14
16
Frequency (GHz)

(a)

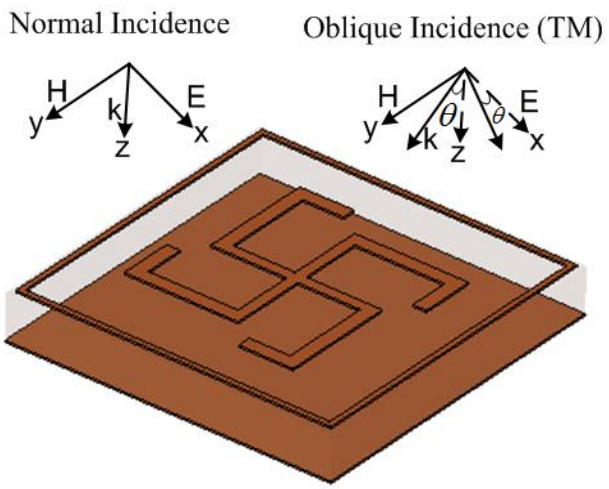
Normal Incidence
Oblique Incidence (TM)
H
E
k
y
x
z
θ

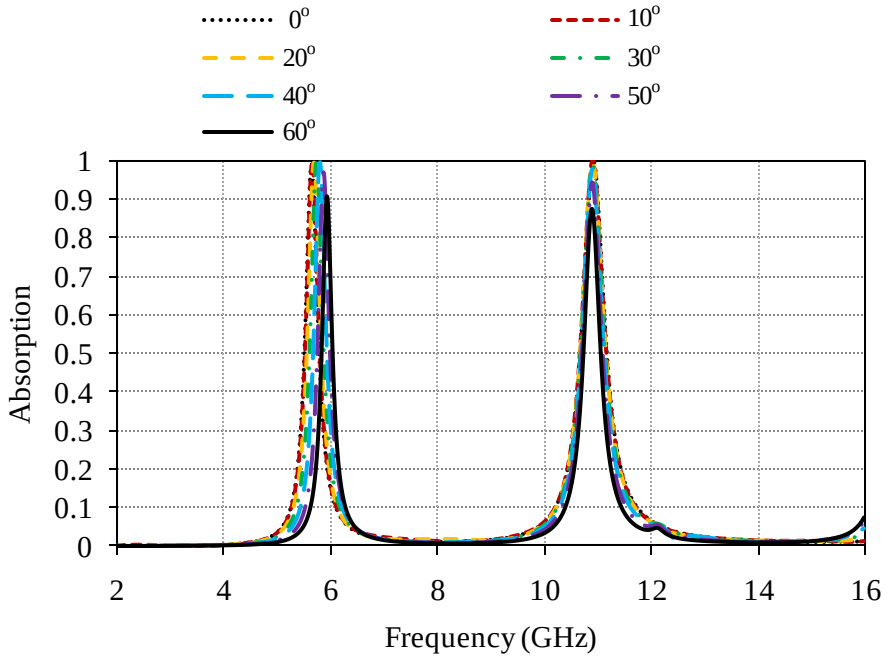

(b)

Figure 3.6 (a) Variation of absorptivity with an incident angle (θ) for TE polarized wave, (b) Variation of absorptivity with an incident angle (θ) for TM polarized wave

The parametric examination of the proposed structure is also carried out and its effect on absorptivity curve is shown in Figure 3.7. The analyses were performed by keeping all parameters fixed while varying only one parameter under 0^o incident angle.

Figure 3.7(a) shows that the width of the outer ring i.e. w_1 is varied keeping all other parameters constant. This shows only a small variation in the absorption peak at the same resonating frequency. The optimized parameters give the highest absorptivity nearly 99.4%.

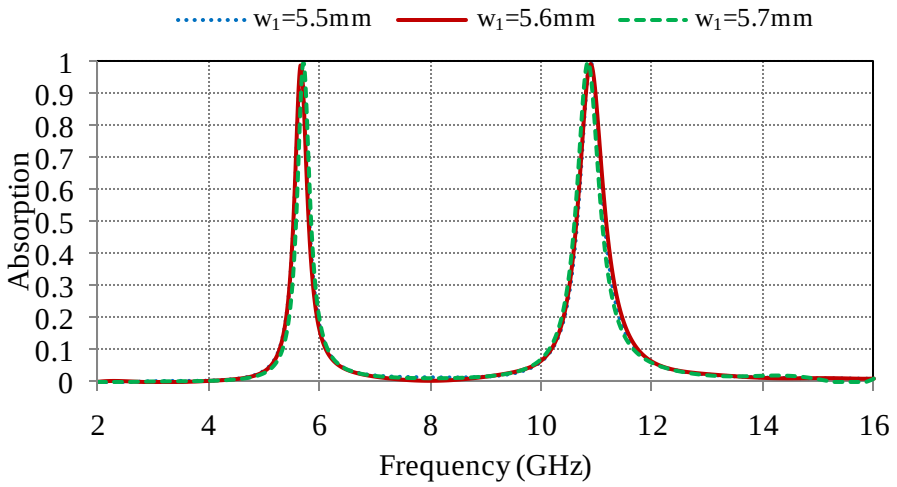

(a)

Further, the effect of variation of the parameter of the swastika-shaped structure on the absorption curve is also studied. The variation of length d of the swastika-shaped geometry is shown in Figure 3.7(b) keeping all other parameters fixed. It is observed from Figure 3.7(b) that the increase in the length of the structure led to increase in the inductance of the structure as a result of which the absorption peak shifts on the way to the lower frequency side. Moreover, the optimized value of the geometry gives the maximum peak absorptivity as compared to the other parameters.

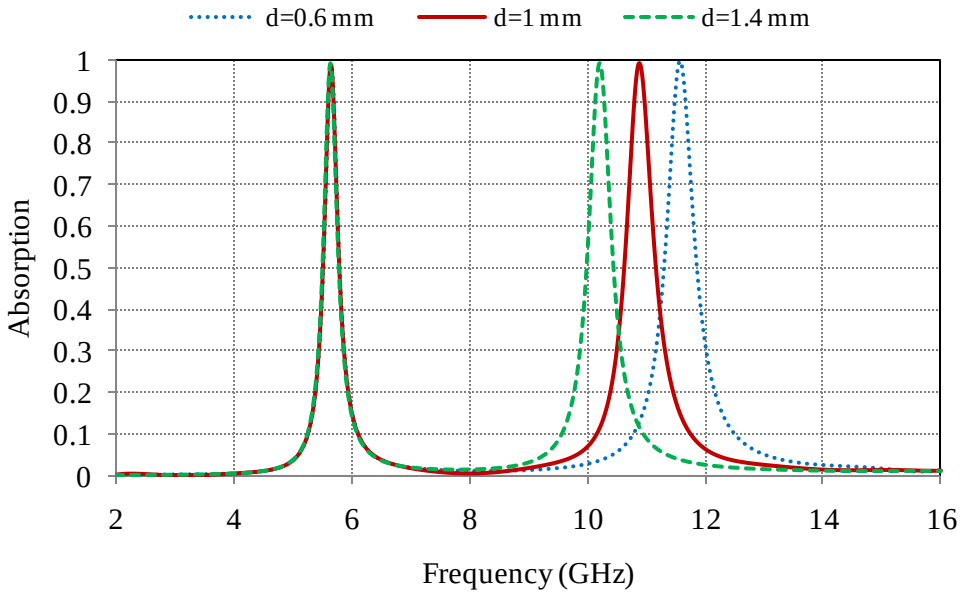

(b)

Further width of the swastika-shaped structure i.e. w_3 is varied keeping all other parameters fixed as shown in Figure 3.7(c). It is noticed that while rising the value of the width of the swastika-shaped geometry, the absorption peak shifts towards the higher frequency side due to the reduction in the corresponding capacitance of the geometry.

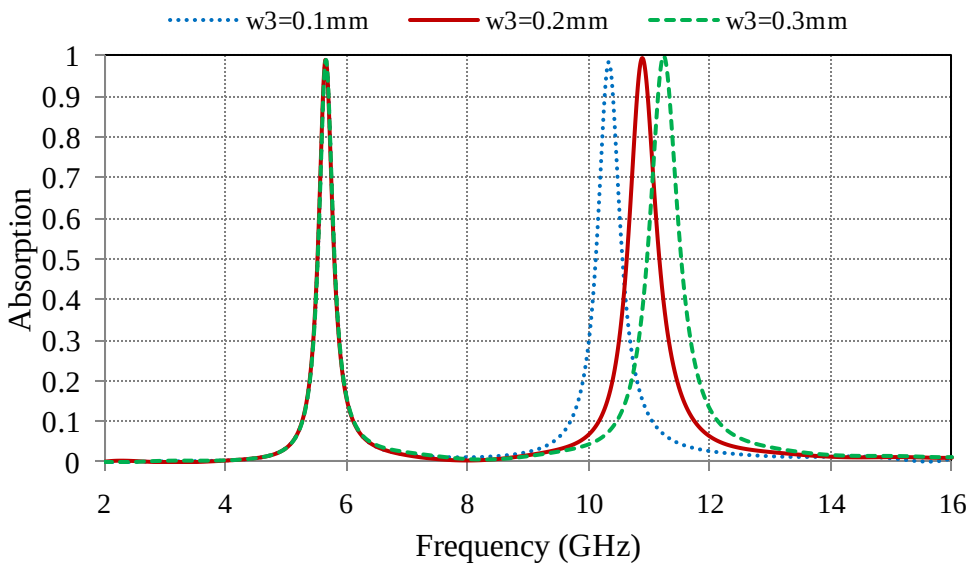

(c)

Figure 3.7 (a) Variation of the width of the outer ring, (b) Variation of the length of the rectangular shape of the inner structure, (c) Variation of the width of the inner structure

3.4 EXPERIMENTAL RESULTS

To obtain the experimental results, a 20 × 20 array of the proposed absorber is fabricated of dimensions 120 × 120 mm^2 and the fabricated absorber design is shown in Figure 3.8(a). The measurement setup of the metamaterial absorber contains a horn antenna, absorber holder and Keysight ENA series network analyzer E5063A (100 kHz-18 GHz). The measurement setup of the proposed metamaterial absorber is given in Figure 3.8(b). The fabricated proposed absorber structure is placed in front of the horn antenna and the reflection coefficient S_{11} is measured and noted. This will show the amount of electromagnetic wave is absorbed by the absorber. This whole measurement operation is done in the free space environment. The comparison of simulated and measured results is shown in Figure 3.8(c).

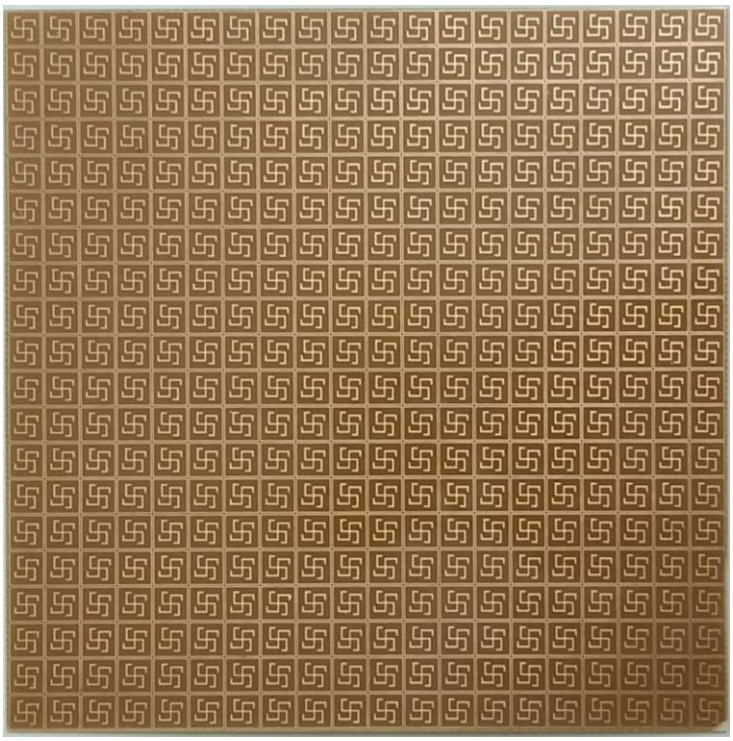

(a)

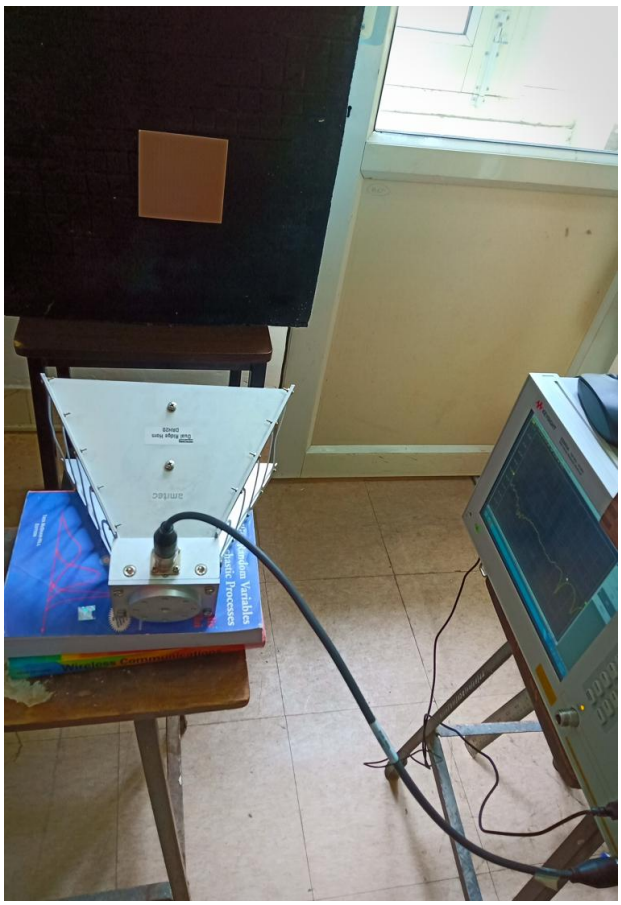

(b)

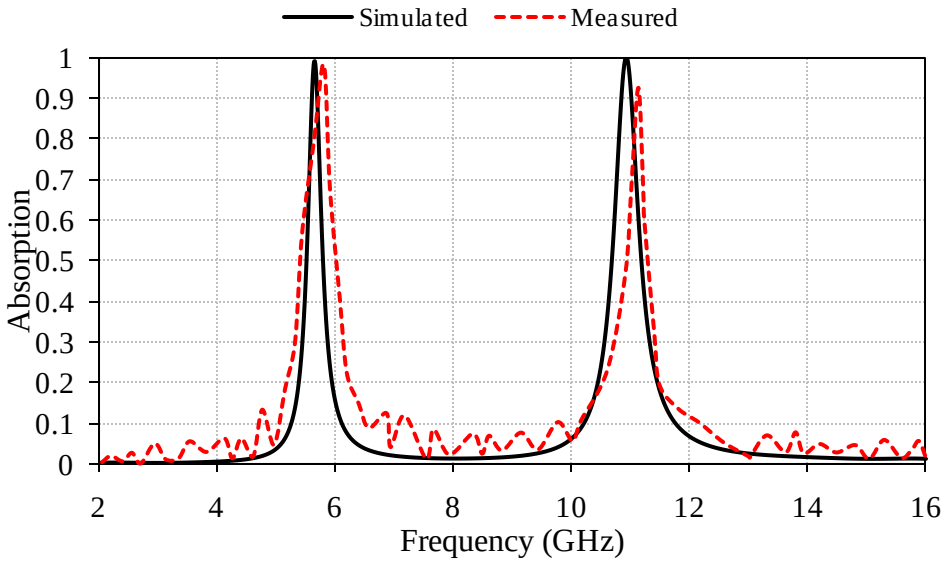

(c)

Figure 3.8 (a) Fabricated absorber design, (b) Measurement setup of the proposed metamaterial absorber, (c) Comparison of simulated and measured results

CHAPTER 4

DESIGN AND ANALYSIS OF A COMPACT ULTRATHIN POLARIZATION- AND INCIDENT ANGLE-INDEPENDENT TRIPLE BAND METAMATERIAL ABSORBER

4.1 INTRODUCTION

This chapter reports a low profile metamaterial absorber with three resonances in S-band, X-band and Ku-band. The geometry of the projected absorber consists of a square ring, a split ring, and a plus-shaped resonating structure. The plus-shaped structure is enclosed within a split-ring resonator and it is further enclosed by an outer square ring. The proposed absorber is engraved on the FR-4 substrate of thickness 1mm i.e. 0.011 λlowest (where λ is the lowest resonating frequency). The size of the unit cell size is 10 × 10 mm^2. It exhibits are 99.6%, 99.1%, and 99.1% absorption at 3.4 GHz, 9.6 GHz, and 13 GHz, respectively. Moreover, the physical insight of the design is explained by surface current distribution and equivalent circuit analysis. Stability of the proposed design is validated with different incident (for TE and TM modes) angles and different polarization angles. Finally, a replica of the absorber is fabricated and validated experimentally. The pictorial view of the surface current distribution illustrates the resonating mechanism of the absorber.

4.2 ABSORBER CONFIGURATION AND DESIGN METHODOLOGY

The projected absorber consists of three layers namely the top layer (resonating structure), bottom layer (metallic ground plane), and a dielectric layer. The 3D perspective view of the proposed absorber is represented in Figure 4.1(a) and details of design parameters are represented in Figure 4.1(b). The top and bottom layers are made of copper (thickness 35μm and conductivity $\sigma = 5.96\times10^7$ S/m). FR4 substrate (ε_r=4.4 and tanδ=0.018) is used as a dielectric layer with 1mm thickness i.e. 0.011 λ_{lowest} (where, λ is the lowest resonating frequency). It is considered a middle layer that is stuck between the top and bottom metallic layers. The top electric resonator consists of three different geometrical configurations. The plus-shaped resonating structure is placed within a split-ring resonator and it is further enclosed by an outer square ring. Full-wave simulations and optimizations of the metamaterial absorber are carried out using finite integration technique (FIT) based computer simulation microwave studio (CST MWS) with periodic boundary conditions. However, the

absorptivity $A(\omega)$ of the metamaterial absorber is calculated by using the formula as given in the appendix.

The proposed absorber is designed in such a way that each resonating structure resonates at a particular frequency. The design methodology of the proposed absorber can be interpreted in three geometrical steps as shown in Figure 4.2(a). The absorption response corresponding to each configuration is presented in Figure 4.2(b).

At first, each individual geometry and its corresponding absorption is analyzed as shown in Figure 4.2. It is noted that each geometry is responsible for the absorption at a different frequency. However, they do not give adequate absorptivity individually. Further, a combination of two or more geometries and their absorptivity are analyzed as presented in Figure 4.3. It is observed that when two adjacent geometries are combined with each other, absorptivity increases remarkably because of the mutual coupling between the geometries. From Figure 4.2(b), it is noticed that the Absorber-B individually gives very less absorptivity of only 82.5% at 13 GHz. But when this Absorber-B geometry is combined with Absorber-A geometry then it can give strong absorption of 95.9% at the same resonating frequency i.e. 13 GHz with an additional resonance at 3.42 GHz with peak absorptivity of 99.5% as shown in Figure 4.3(a). Similarly, when all the three individual geometries are combined (proposed absorber), nearly perfect absorption is obtained at 3.42 GHz, 13 GHz along with one more absorption peak at 9.61 GHz as shown in Figure 4.3(b). Moreover, the surface current distribution is also provided to verify the behavior of geometries. It is noted from Figure 4.4 that at the resonating frequency of 3.42 GHz, surface current is more concentrated at outer ring thus it means that Absorber-A is liable for the absorption at 3.42 GHz, whereas at higher frequency i.e. 13 GHz the surface current distribution is more dense at the split ring resonating structure, therefore, the absorption at 13 GHz is mainly due to the split ring structure (Absorber-B) and at 9.61 GHz the surface current distribution has more strength at the inner plus-shaped geometry thus it means that the Absorber-C is largely responsible for the absorption at 9.61 GHz.

Table 4.1 Design Parameters of Absorber

Parameters	Size (mm)	Parameters	Size (mm)
A	10	g	0.8
B	9.8	l_1	4
W_1	0.65	W_3	0.36
D	7.8	l_2	2
W_2	0.4	W_4	0.18

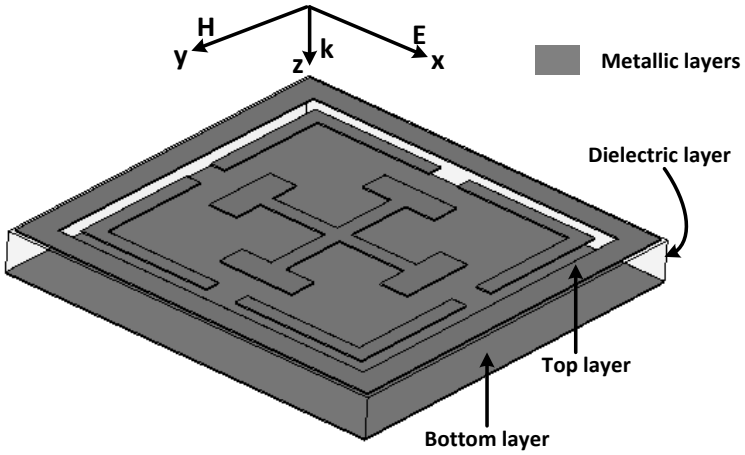

(a)

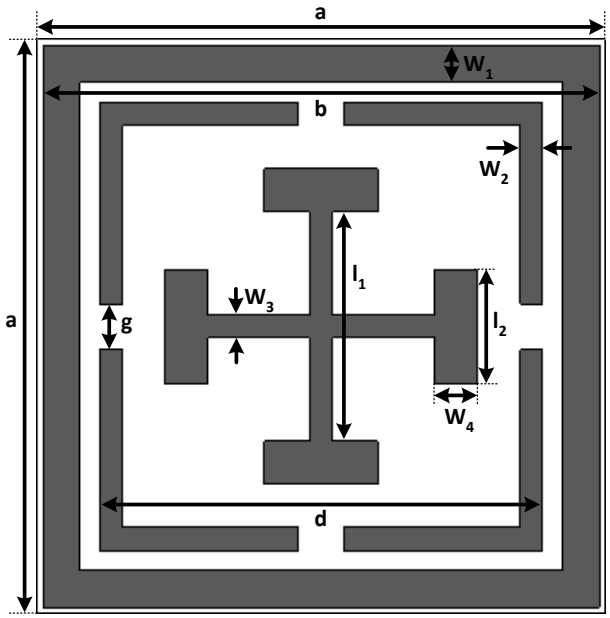

(b)

Figure 4.1 (a) Perspective view of the proposed absorber, (b) Detailed dimensions of proposed absorber

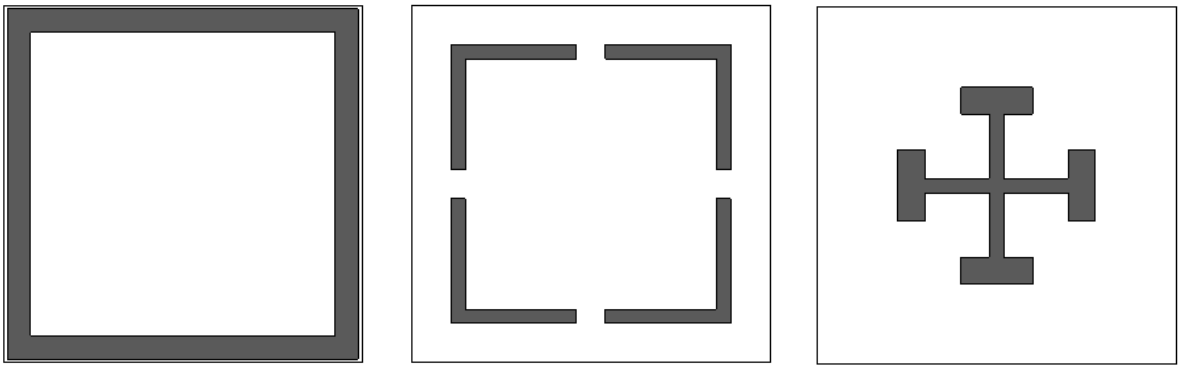

Absorber-A **Absorber-B** **Absorber-C**

(a)

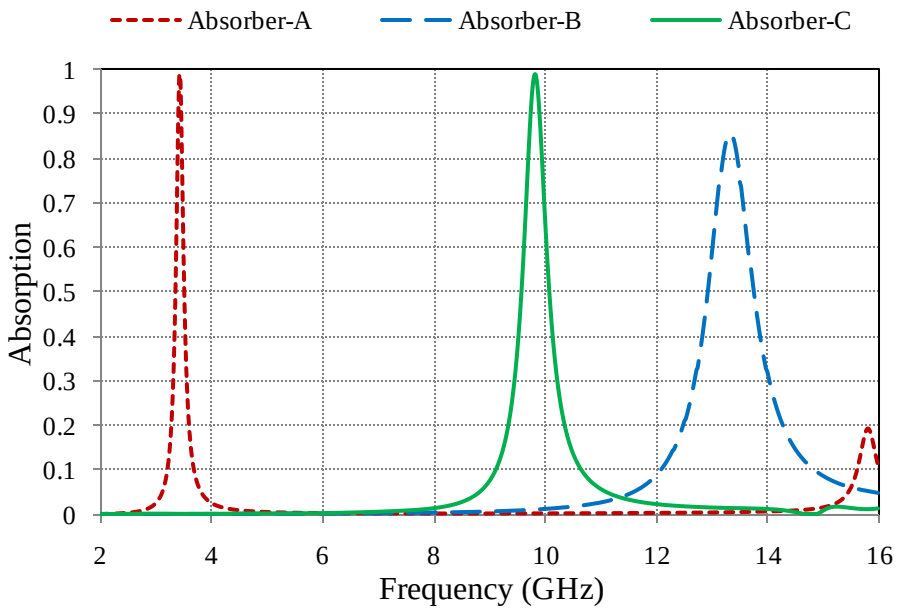

(b)

Figure 4.2 (a) Individual geometries of the proposed absorber, (b) Absorptivity curve corresponding to each individual geometry

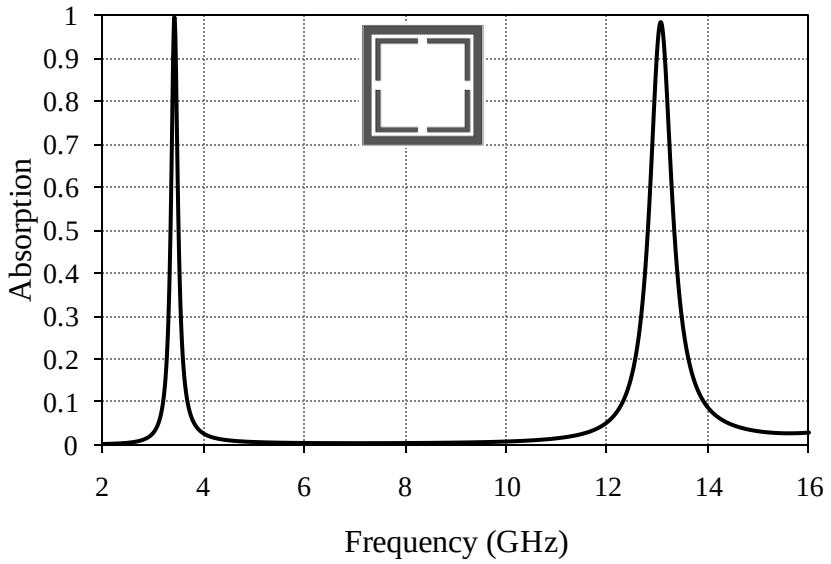

(a)

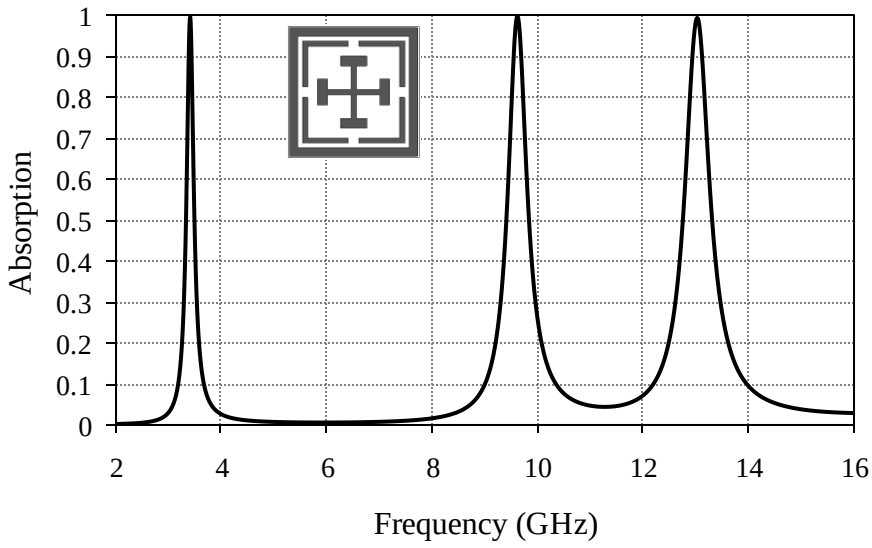

(b)

Figure 4.3 (a) Absorptivity curve of absorber-D, (b) Absorptivity curve of the proposed absorber

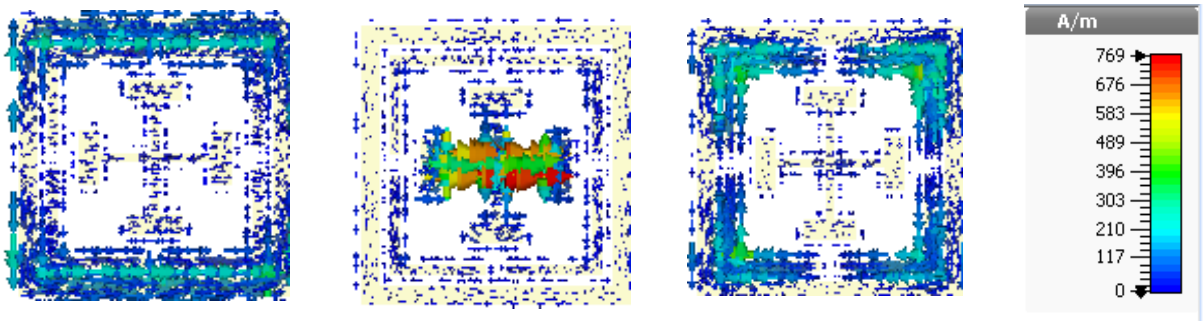

3.42 GHz 9.61 GHz 13 GHz

Figure 4.4 Surface current distribution

4.3 RESULTS AND DISCUSSIONS

CST MWS [28] is used to carry out all the simulations. The proposed absorber is observed under both transverse electric (TE) and transverse magnetic (TM) modes and it provides the same level of absorptivity under both modes as shown in Figure 4.5. Further, the polarization sensitivity of the proposed absorber is studied under oblique and normal angles of incidence for Transverse Electric (TE) mode. The directions of magnetic field and wave vector are changed keeping the direction of electric field constant to analyze the absorptivities under oblique incidence and direction of wave propagation is made normal along z-direction while changing the directions of electric field and magnetic field to test the polarization behavior of the structure under normal incidence. The design is showing no variation while varying the polarization angles thus making it polarization-insensitive in nature due to its symmetry in structure as shown in Figure 4.6.

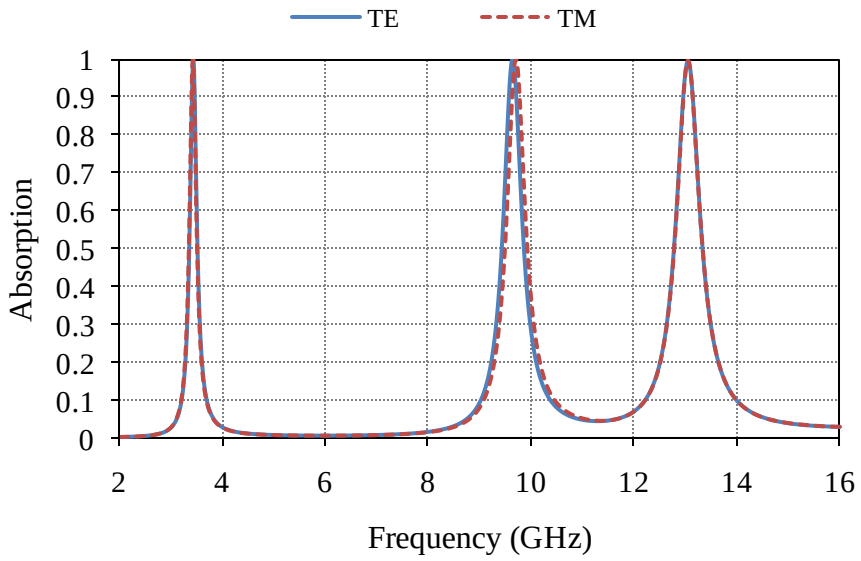

Figure 4.5 Absorptivity curve under TE and TM modes

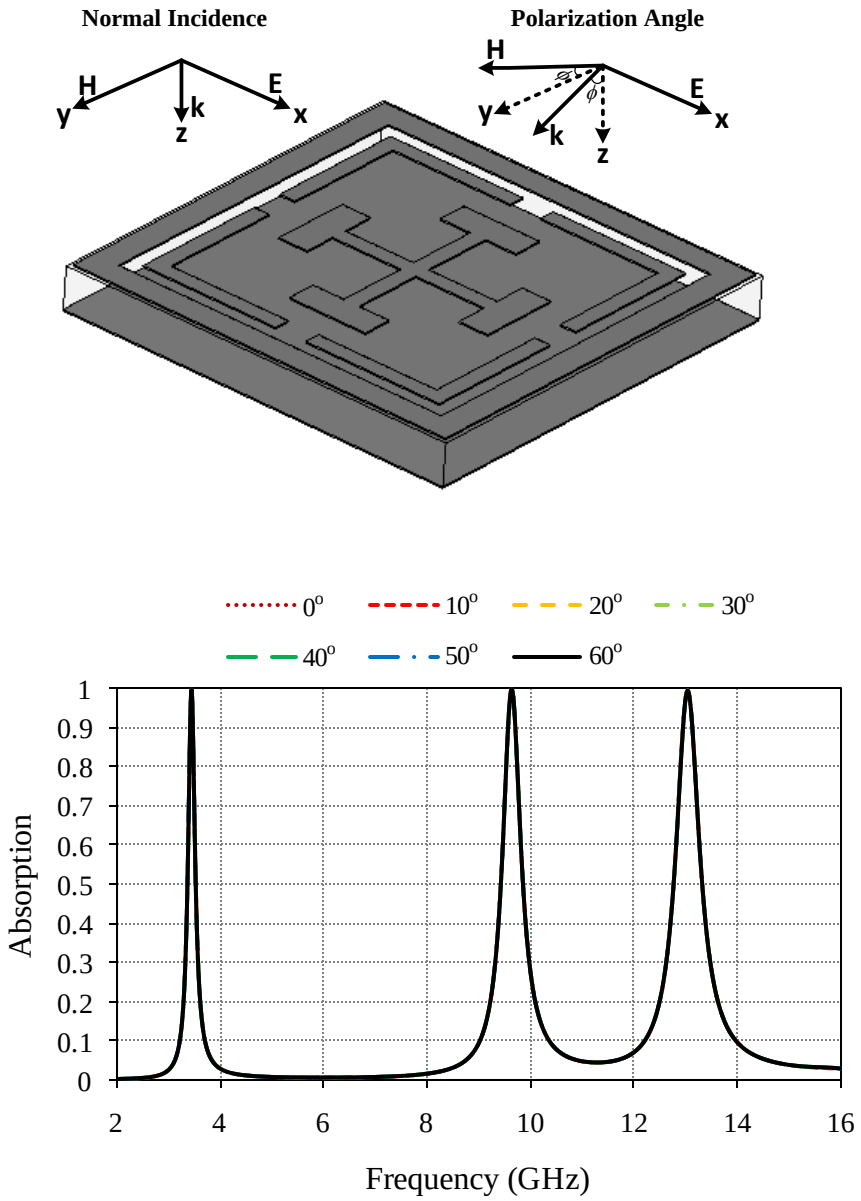

Figure 4.6 Variation of absorptivity with polarization angle (ϕ)

Further, incident angle variation is done to observe its effect on the absorptivity curve as shown in Figure 4.7. Firstly, magnetic field and wave vector directions are varied by an angle θ while keeping the electric field direction constant as shown in Figure 4.7(a). Then, the electric field and wave vector directions are varied by an angle θ while keeping the magnetic field direction constant as shown in Figure 4.7(b). It is observed from the results that as we are changing the incident angle from normal to oblique, the slight variations in the absorption peaks along with small side peaks have occurred.

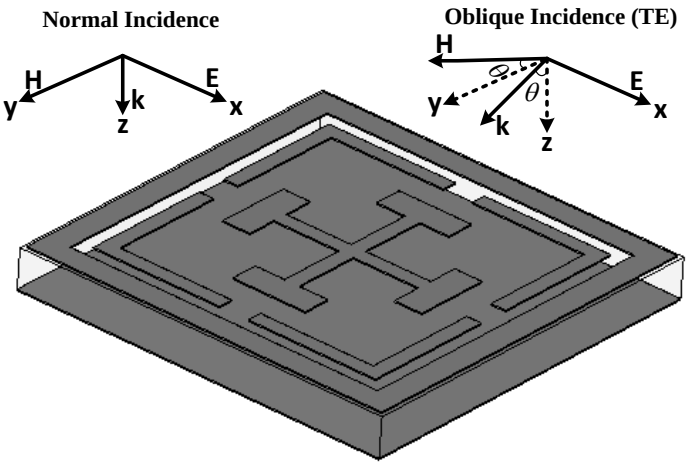
Normal Incidence
Oblique Incidence (TE)
H
E
k
y
x
z
θ

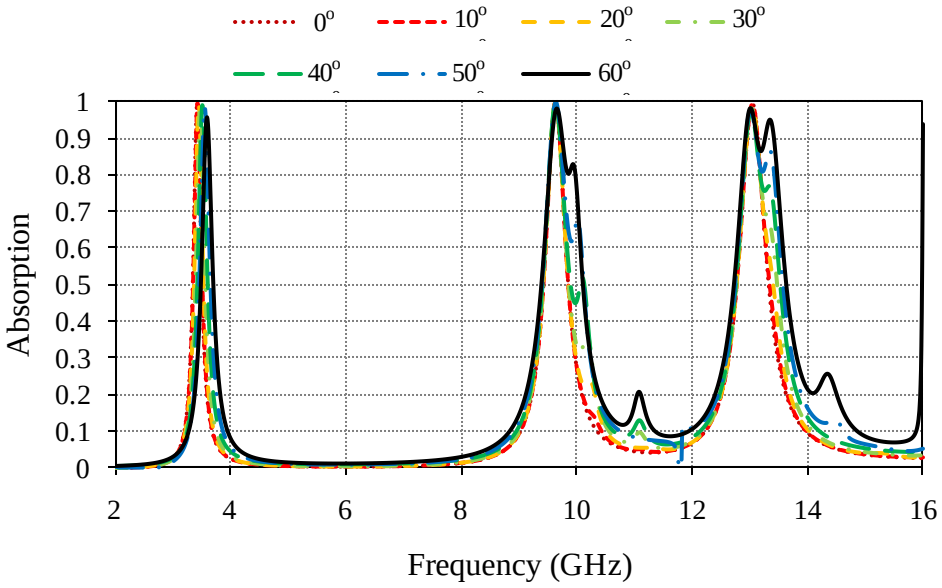
0°
10°
20°
30°
40°
50°
60°
Absorption
Frequency (GHz)
0
0.1
0.2
0.3
0.4
0.5
0.6
0.7
0.8
0.9
1
2
4
6
8
10
12
14
16

(a)

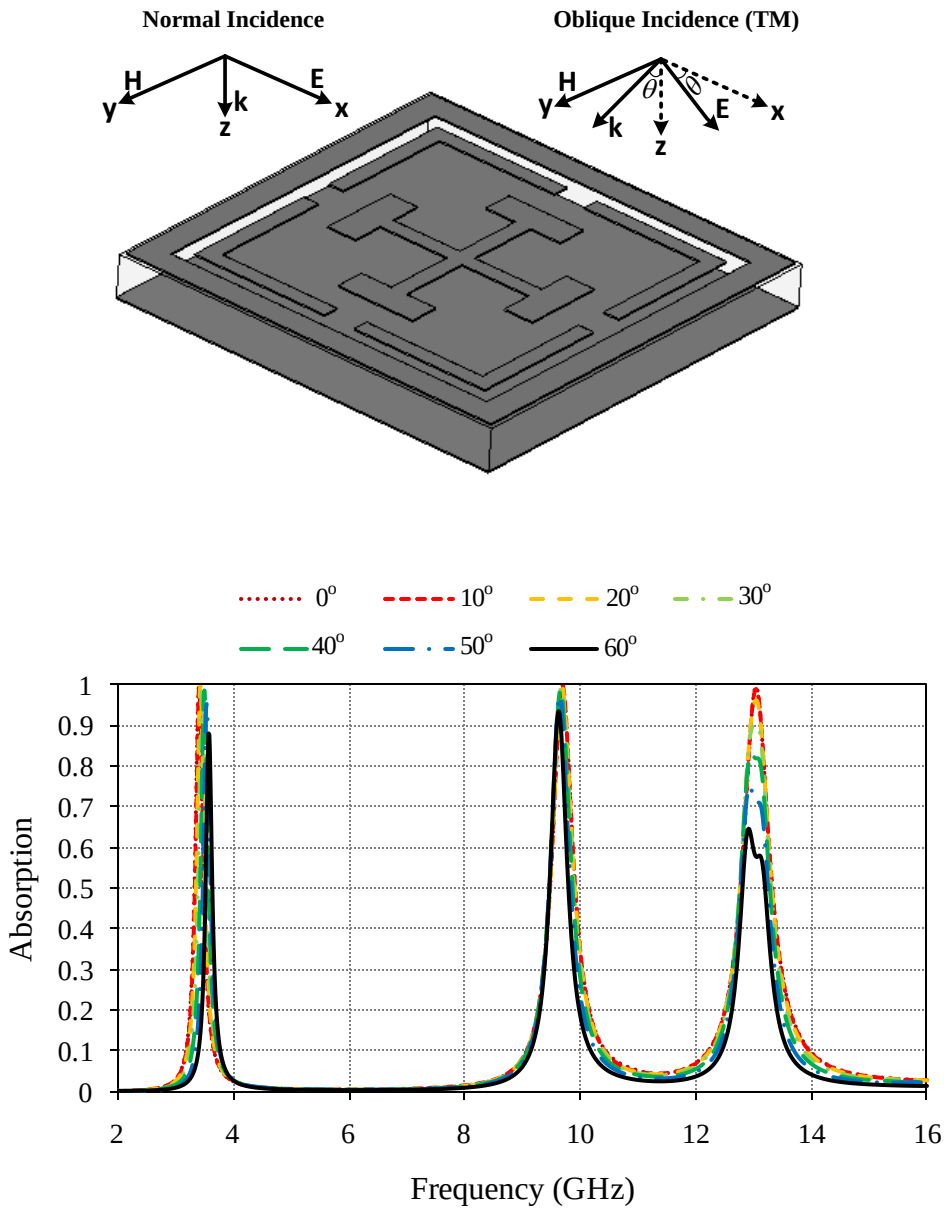

(b)

Figure 4.7 (a) Variation of absorptivity with incident angle (θ) for TE polarized wave, (b) Variation of absorptivity with incident angle (θ) for TM polarized wave

4.4 EXPERIMENTAL RESULTS

To obtain the experimental results, a 10 × 10 array of the proposed absorber is fabricated of dimensions 100 × 100 mm^2 and the fabricated absorber design is shown in Figure 4.8(a). The measurement setup of the metamaterial absorber contains a horn antenna, absorber holder and Keysight ENA series network analyzer E5063A (100 kHz-18 GHz). The measurement setup of the projected metamaterial absorber is presented in Figure 4.8(b). Firstly, a copper sheet of the same size is positioned in front of the horn antenna and the reflection coefficient S_{11} is measured. Then, the

fabricated proposed absorber structure is placed in front of the horn antenna and the reflection coefficient S_{11} is measured. This is done to normalize the reflectance from the absorber structure concerning the reflectance from the copper sheet. This whole measurement operation is done in the free space environment. A comparison of simulated and measured results is shown in Figure 4.8(c).

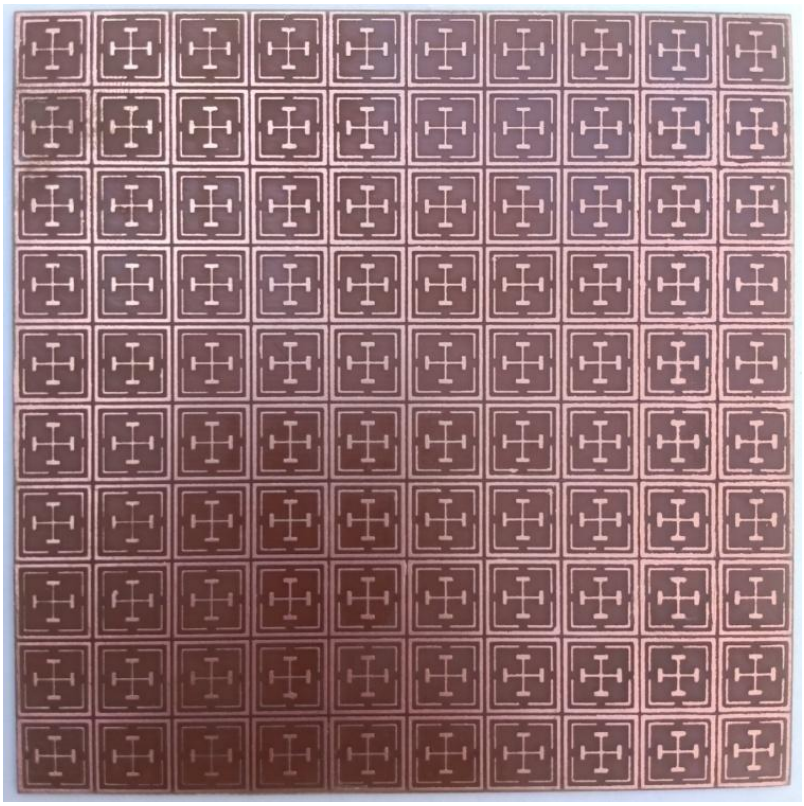

(a)

(b)

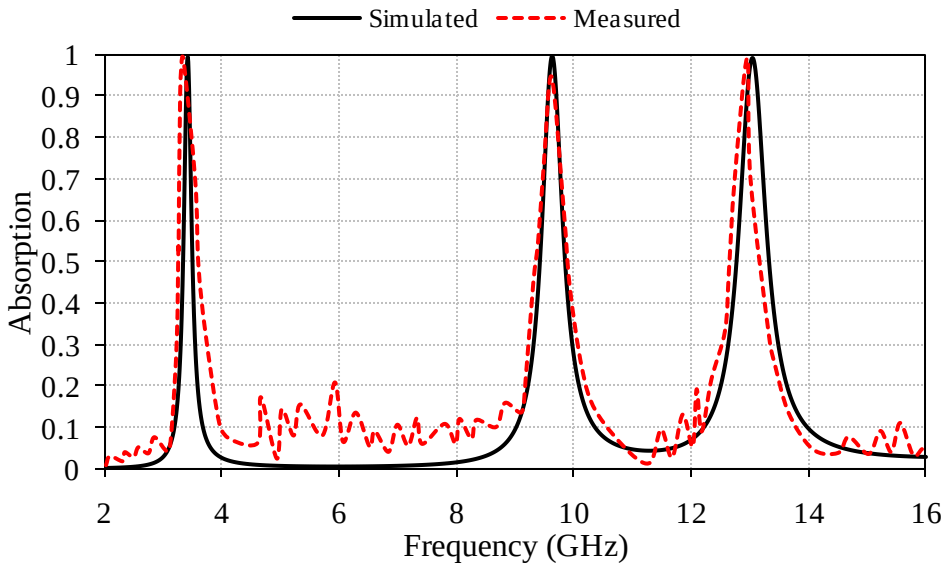

(c)

Figure 4.8 (a) Fabricated absorber design, (b) Measurement setup of the proposed metamaterial absorber, (c) Comparison of simulated and measured results

CHAPTER 5
A COMPACT METAMATERIAL BASED WIDEBAND ABSORBER

5.1 INTRODUCTION

Many metamaterial absorbers have been proposed till date but they suffer from the drawback of having a narrow bandwidth. Many designs have been proposed in which wideband absorption is achieved by using multiple dielectric layers but their huge thickness becomes a big constraint in many applications. In this chapter, an ultrathin wideband metamaterial has been projected. Wideband absorption is achieved when multiple resonating structures resonating at different resonating frequencies come closer to each other and thus provides wide bandwidth. The projected structure includes an L-shaped structure and a diagonal rectangular shaped structure. The dimension of the unit cell arrangement is 5×5 mm^2 and the thickness of the structure is 1.54mm. The proposed structure provides the wideband absorptivity of 9 GHz from 12 GHz to 21 GHz having absorption of 99.6%, 99.9%, and 97.6% at three resonating frequencies i.e. 12 GHz, 17 GHz, and 21 GHz respectively. The proposed provides the same absorptivity for the different polarization angles thus making it polarization-insensitive in nature. Moreover, the structure is also studied for different incident angles for both transverse electric (TE) and transverse magnetic (TM) modes.

5.2 CONFIGURATION AND DESIGN OF PROPOSED ABSORBER

The detail dimensions of the proposed wideband metamaterial absorber structure are given in Figure 5.1(a). This wideband absorber structure has 3 layers. The top layer includes a metallic patch (design) and the bottom layer includes a metallic ground formed of copper with a thickness of 0.035mm and conductivity $\sigma = 5.96 \times 10^7$ S/m. The middle layer is sited between both metallic layers is a dielectric layer made of the FR-4 substrate having thickness 1.54mm and dielectric constant $\varepsilon = 4.3$. The proposed wideband structure is formed by the combination of two structures i.e. an L-shaped structure and a diagonal rectangular shaped structure. Full-wave simulation of the metamaterial absorber is carried out using finite integration technique based computer simulation microwave studio (CST MWS) with periodic boundary conditions and Floquet port excitations. However, the absorptivity $A(\omega)$ of the metamaterial absorber is calculated by using the formula as given in the appendix. Through the optimization of the parameters of the metamaterial microwave absorber structure, the final parameters are found which are listed below in Table 5.1.

Table 5.1 Design Parameters of Proposed Wideband Absorber

Parameters	Size (mm)	Parameters	Size (mm)
a	5	l	3
b	3.3	w	1.1
c	0.9		

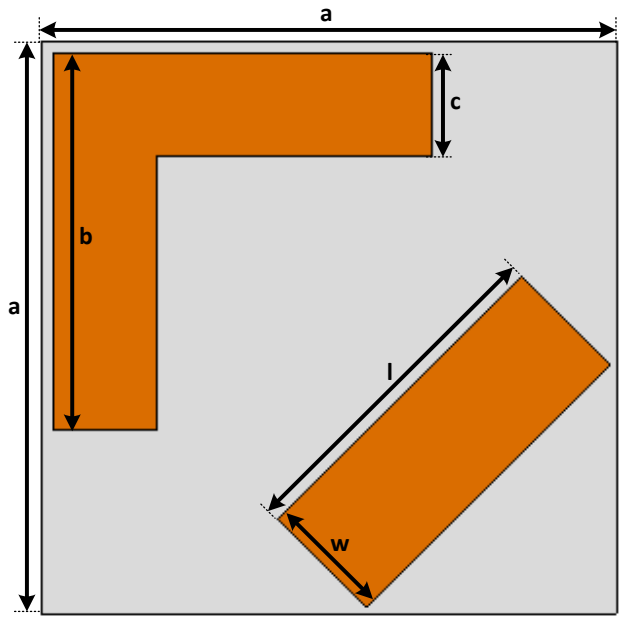

Figure 5.1 Detailed dimensions of the proposed wideband absorber

The proposed design is formed in such a mode that the different structures resonating at different resonating frequencies come closer to each other giving the wideband absorption. The presented absorber design consists of two geometrical structures named as Absorber-A and Absorber-B. This is illustrated below in Figure 5.2(a) and their consequent absorptivity curve is shown in Figure 5.2(b). It is noticed that Absorber-A alone is giving good impedance matching but lacks in providing good wideband absorption and Absorber-B alone is not capable of giving impedance matching. However, the combination of two geometries (proposed absorber) is responsible for giving wideband absorption along with nearly perfect impedance matching of 99.6% at 12 GHz, 99.9% at 17 GHz and 97.6% at 21 GHz as shown in Figure 5.3. Furthermore, the surface current distribution of the proposed wideband absorber at three resonance peaks is shown in Figure 5.4 for better visualization of the structure. It is noted that the mutual coupling between the two geometries provides better impedance

matching along with the bandwidth enhancement of the structure giving wideband absorbance of 9 GHz from 12 GHz to 21 GHz frequency range.

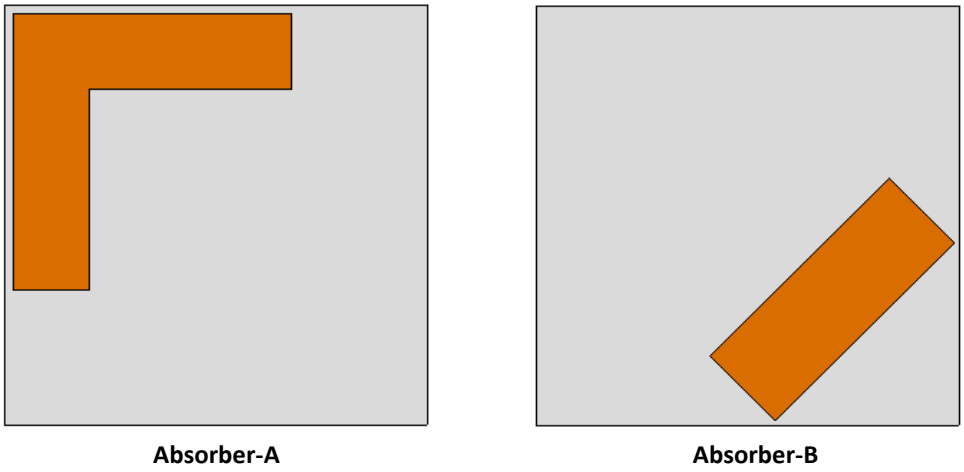

(a)

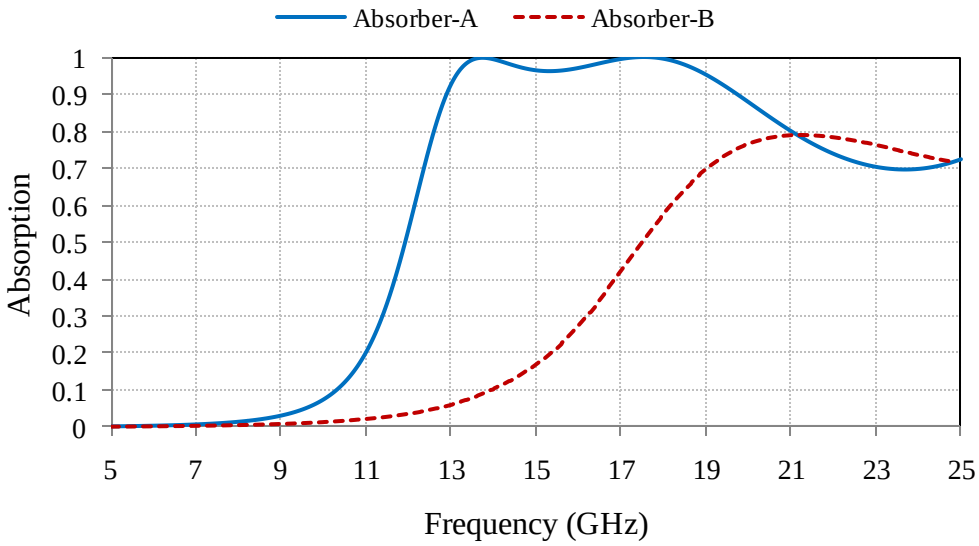

(b)

Figure 5.2 (a) Individual geometries of the proposed wideband absorber, (b) Absorptivity curve corresponding to each individual geometry

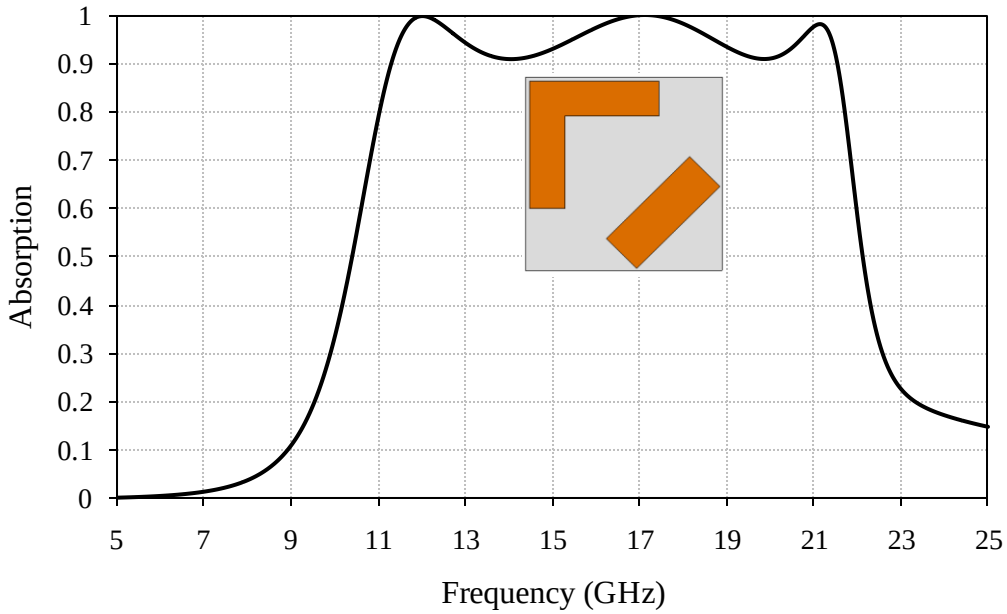

Figure 5.3 Absorptivity curve of the proposed absorber

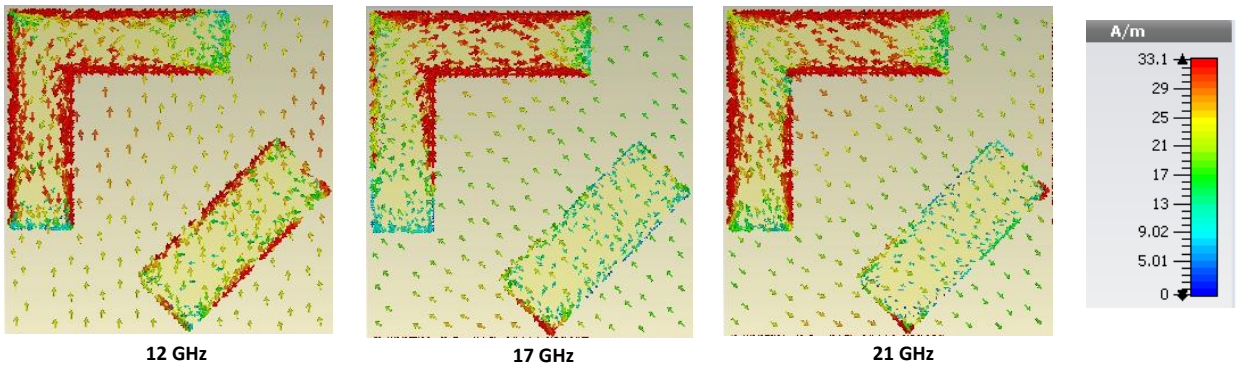

Figure 5.4 Surface current distribution

5.3 RESULTS AND DISCUSSIONS

All the simulations have been accomplished using CST MWS. Normal angle and oblique angles of incidence are measured to study the polarization dependency of the design. The analysis is carried out by varying the polarization angle keeping the incident angle constant as represented in Figure 5.5. It is noticed that the absorption curves overlapped each other when the polarization angle varies from 0^{o} to 60^{o}. Therefore, no variation at diverse polarization angles making it polarization-insensitive in nature. Further, the variation of absorption with a diverse incident angle is shown in Figure 5.6. It is noticed that the slight variation in the absorption peaks along with small side peaks are occurred as when we are changing the incident angle from normal to oblique.

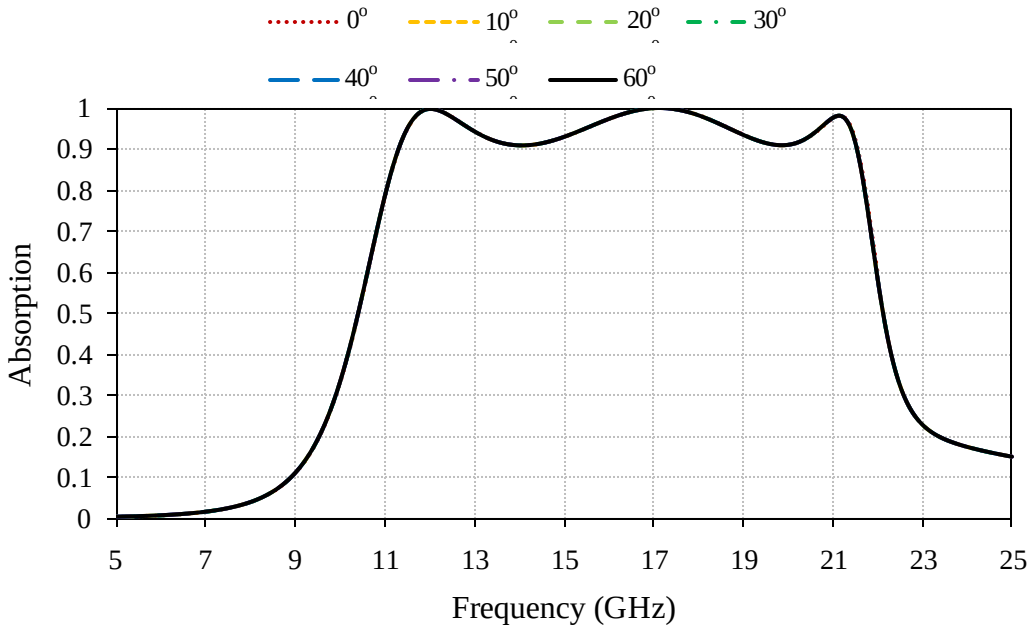

Figure 5.5 Variation of absorptivity with polarization angle (ϕ)

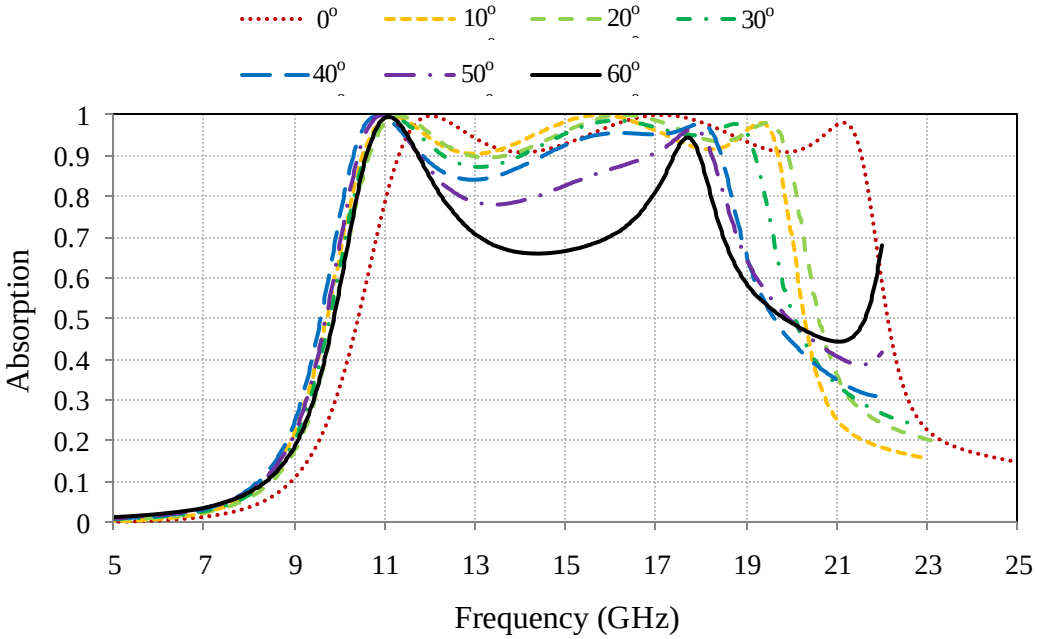

Figure 5.6 Variation of absorptivity with incident angle (θ)

3.5 EXPERIMENTAL RESULTS

To obtain the experimental results, a 40 × 40 array of the proposed absorber is fabricated of dimensions 200 × 200 mm^2 and the fabricated absorber design is shown in Figure 5.7(a). The measurement setup of the metamaterial absorber contains a horn antenna, absorber holder and Keysight ENA series network analyzer E5063A (100 kHz-18 GHz). The measurement setup of the projected metamaterial absorber is presented in Figure 5.7(b). The fabricated proposed absorber structure is positioned in front of the horn antenna and the reflection coefficient S_{11} is measured and noted. This will show the amount of electromagnetic wave is absorbed by the absorber. This whole measurement operation is done in the free space environment. A comparison of simulated and measured results is shown in Figure 5.7(c).

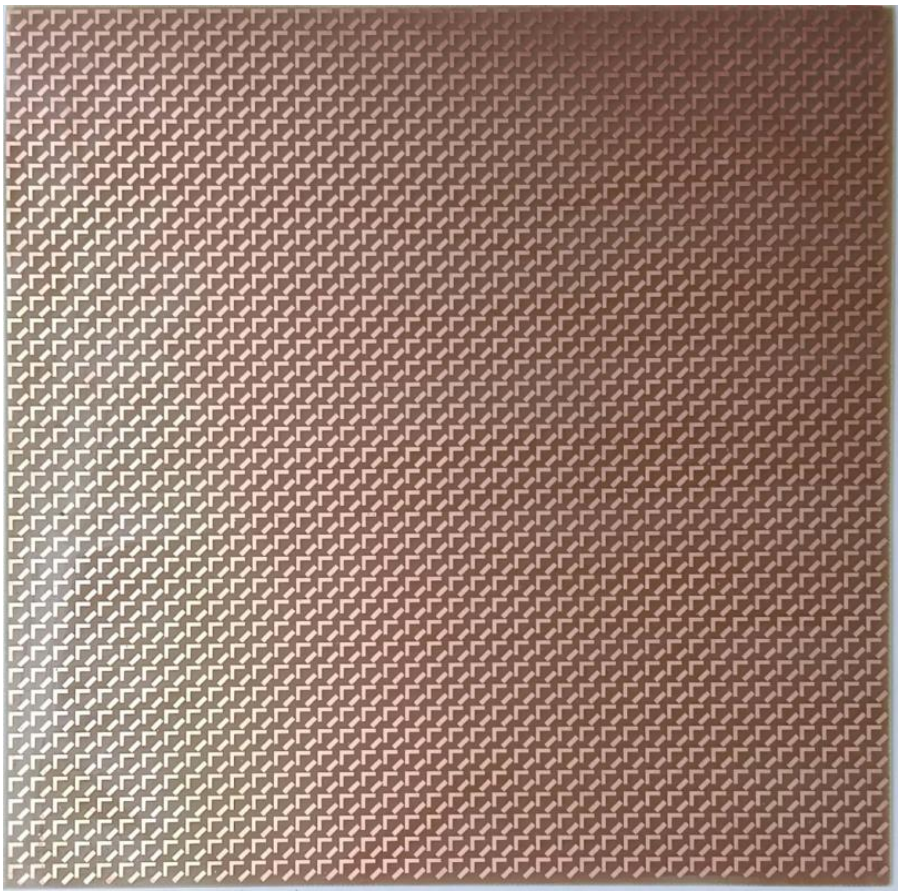

(a)

(b)

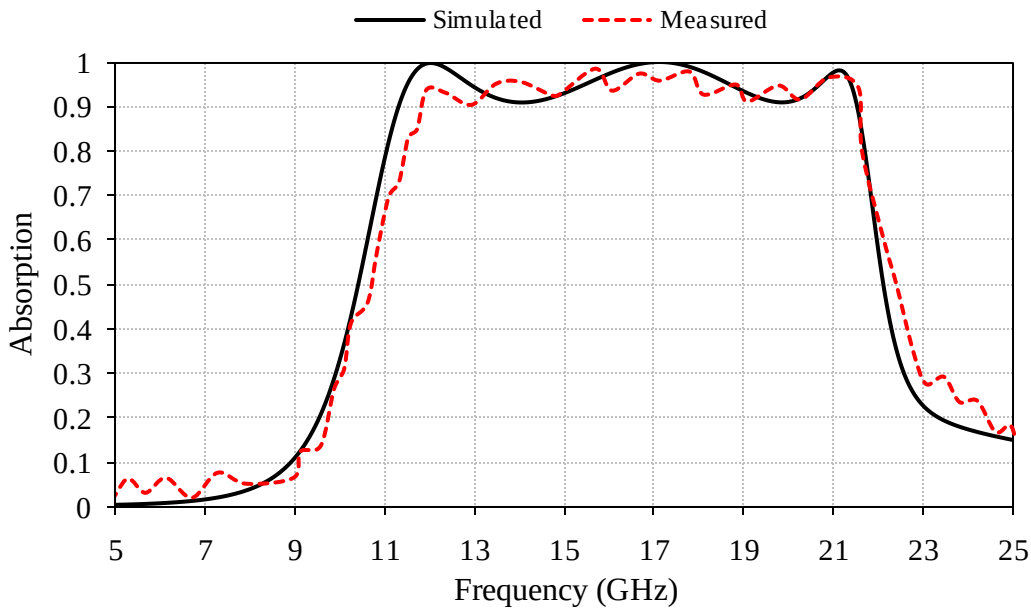

(c)

Figure 5.7 (a) Fabricated absorber design, (b) Measurement setup of the proposed metamaterial absorber, (c) Comparison of simulated and measured results

CHAPTER 6

ISOLATION IMPROVEMENT OF THE MIMO PIFA USING METAMATERIAL ABSORBER ARRAY

6.1 INTRODUCTION

Nowadays, the high quality and high-performance demands have been increased which led the researchers to investigate new multi-input and multi-output (MIMO) antennas. In this chapter, a planar inverted-F antenna (PIFA) has been presented for the use in mobile handsets with high remoteness between the antenna components. Various methods have been employed till now to provide isolation between the antenna elements like to bound the radiation in the propagating direction and to enlarge the distance between the antennas. However, this method is not so proficient as the antenna elements have a very small area in mobile devices. In this chapter, the isolation between the PIFA antenna components is provided using the array of the metamaterial unit cell within the center of the two antenna components. The proposed structure consists of two antenna components with swastika-shaped design on the FR-4 substrate having dimensions of 7 × 7 × 0.8 mm^3. These two antenna elements are formed on the FR-4 substrate of dimensions 100 × 50 × 0.8 mm^3 at a height of 2.8mm from the ground surface. The isolation within each antenna element is due to the array of the metamaterial unit cell and each unit cell has dimensions 6 × 6 × 0.8 mm^3. More than -24dB isolation is provided by the 4 × 4 array of the metamaterial absorber at the frequency of 5.65 GHz. Moreover, the shorting pin is used at one edge of the design and the feed point is placed in between the shorting pin and the open edge. The impedance matching of the design can be enhanced by varying the distance between the shorting pin and the feed point. The proposed structure is fed by using a coaxial probe having an impedance of 50 ohms.

6.2 CONFIGURATION AND DESIGN OF PROPOSED ABSORBER

The 3D configuration of the projected geometry is depicted in Figure 6.1(a) whereas the front view and the back view of the proposed MIMO-PIFA are depicted in Figure 6.1(b). The proposed PIFA structure is having the swastika-shaped structure at the front side of the substrate (mobile phone PCB) whereas an array of metamaterial absorber placed at the bottom of the PCB. The unit cell of metamaterial absorber is a combination of two structures i.e. a swastika-shaped enclosed within the square ring structure. The projected antenna elements geometry is designed on the FR-4 substrate having dimensions of 7 × 7 × 0.8 mm^3 at a height of 2.8 mm from the ground plane of dimensions 100 × 50 × 0.8 mm^3. Two PIFAs are placed back to back over mobile phone PCB to make MIMO

configuration. Further, an array of 4 × 4 metamaterial absorber is designed and placed between MIMO elements to obtain high isolation between the multiple antenna elements. Full-wave simulation of the PIFA structure having coaxial probe feeding is carried out using finite integration technique based computer simulation microwave studio (CST MWS). The optimized parameters of the antenna and absorber are listed below in Table 6.1 and Table 6.2, respectively and their detailed dimension structures are depicted in Figure 6.2(a) and Figure 6.2(b) respectively.

Table 6.1 Design Parameters of Antenna Element

Parameters	Size (mm)	Parameters	Size (mm)
a	7	w_1	0.51
b	3.1	w_2	0.45
c	2.7		

Table 6.2 Design Parameters of Metamaterial Absorber Unit Cell

Parameters	Size (mm)	Parameters	Size (mm)
a	6	w_2	0.25
b	5.6	l_1	1.9
w_1	0.1	l_2	3
d	1		

(a)

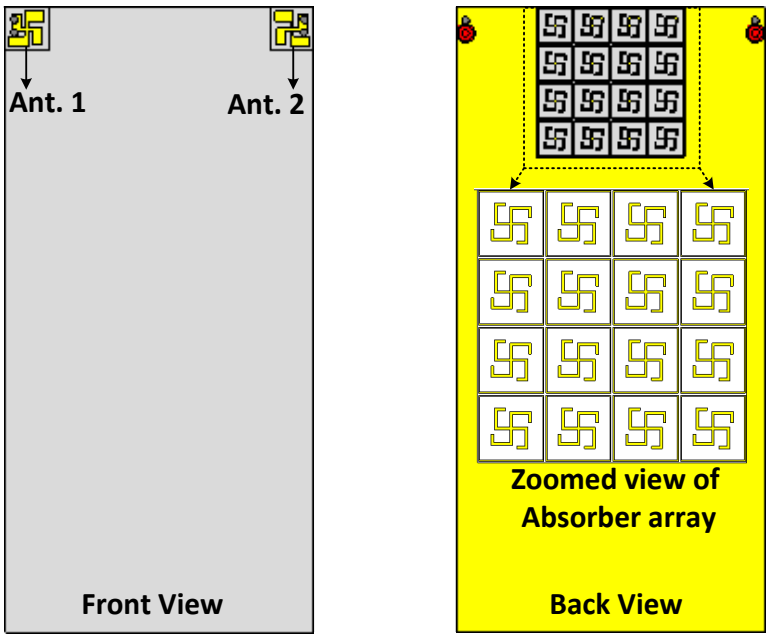

(b)

Figure 6.1 (a) 3D view of the PIFA, (b) Front and back view of the PIFA

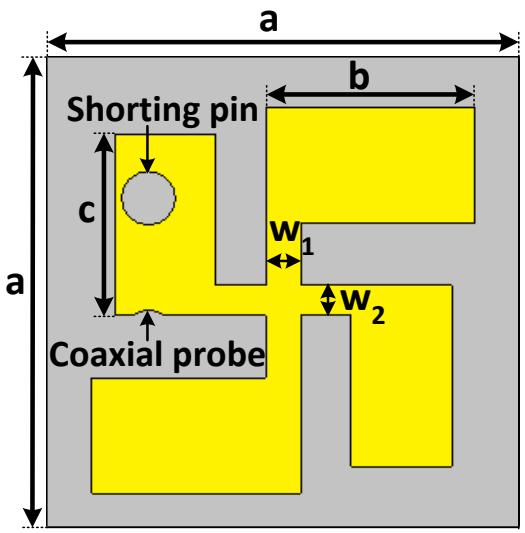

(a)

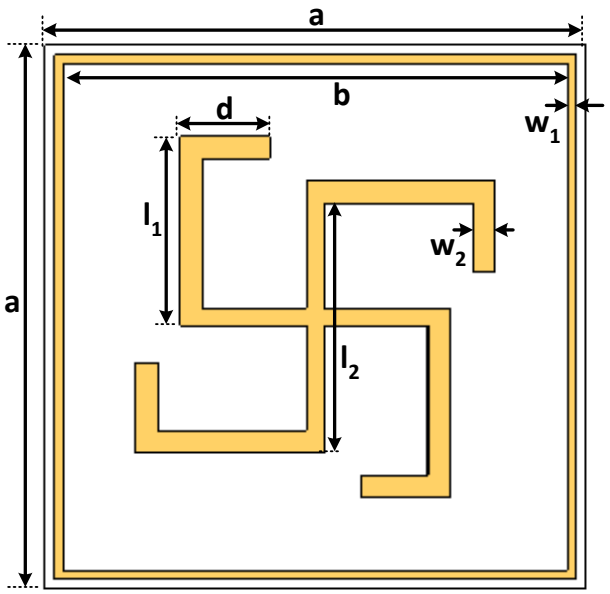

(b)

Figure 6.2 (a) Detailed dimensions of the antenna element, (b) Detailed dimensions of the metamaterial absorber unit cell

6.3 RESULTS AND DISCUSSIONS

6.3.1 S-parameter analysis

All the simulations have been accomplished using CST MWS. The proposed structure includes a metamaterial absorber unit cell which is resonating at 5.65GHz with maximum absorptivity of 98.8%. A 4 × 4 array of the metamaterial absorber is engraved on the back portion of the substrate (mobile phone PCB) within the ground plane to isolate the MIMO antenna elements. The effect of isolation technique (using metamaterial absorber) is shown in Figure 6.3. The reflection coefficients (S_{11} and S_{22}) and transmission coefficients (S_{12} and S_{21}) between two elements will be the same due to the symmetry of the structure, therefore no need to show individual results. It is interestingly noticed that isolation technique (4 × 4 array of absorber) does not make any significant effect on the reflection coefficient, however, the isolation between two elements is drastically increased from -12dB to -25dB at 5.65 GHz. Approximately 13dB enhancement in the isolation is observed.

Furthermore, the effect of isolation technique is optimized from course design to fine design. Initially, the only slot is created between antenna elements. The isolation is increased from -12dB to -16dB, only 4dB isolation enhancement is observed. After that, simulated microwave absorber which resonates at 5.65GHz as shown in Figure 6.4(a) is placed in the slot. Hence, the maximum amount of surface current is now absorbed by the absorber, the result is high isolation is obtained as shown in

Figure 6.4(b). The maximum isolation is -25dB due to a proposed technique which is sufficient to de-correlate the incoming signal at the receiving terminal of the mobile phone.

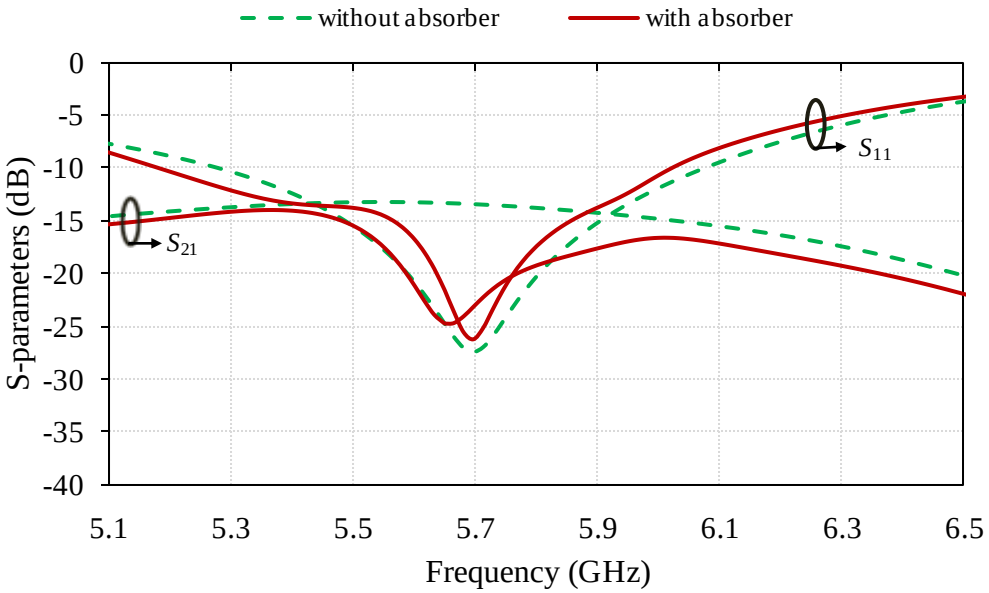

Figure 6.3 S-parameters of the PIFA with and without the absorber array

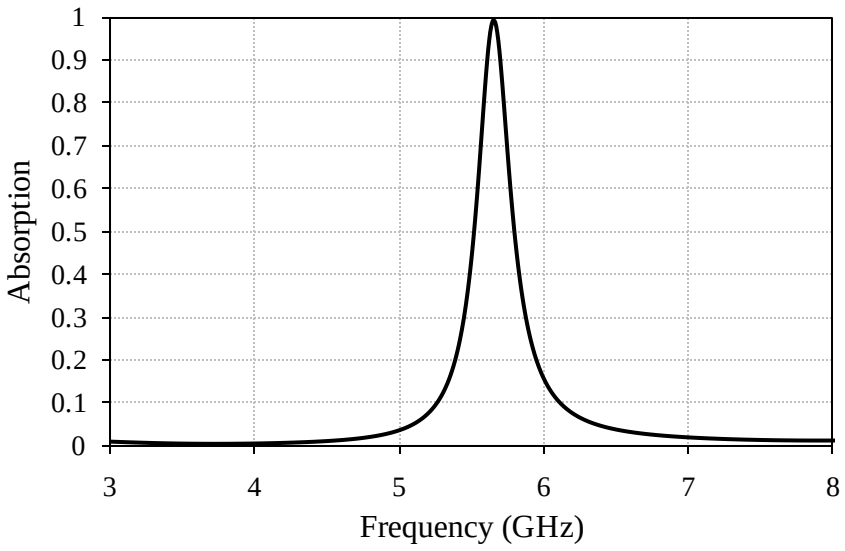

(a)

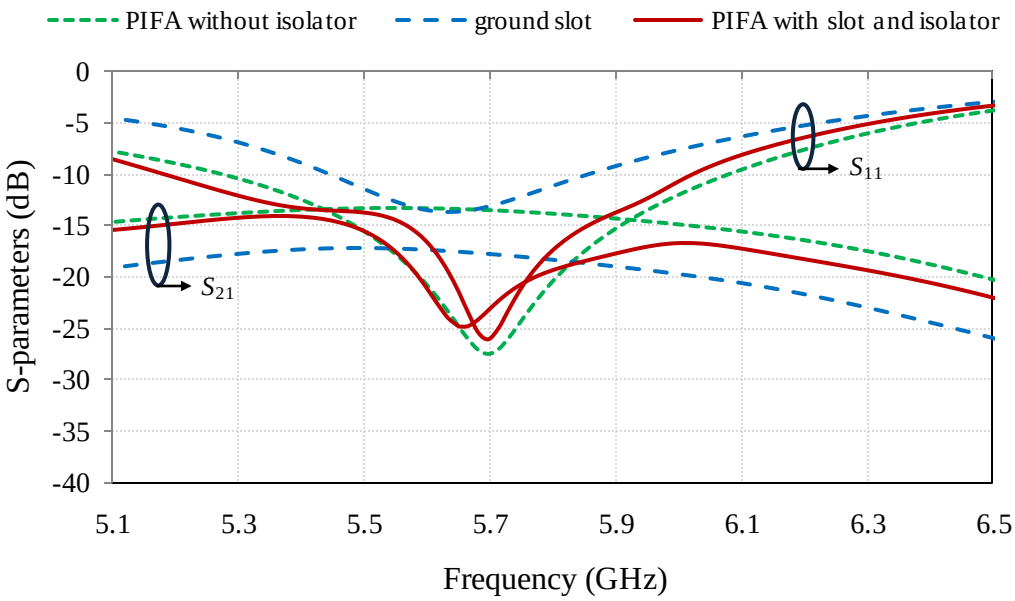

(b)

Figure 6.4 (a) Absorption characteristics of the proposed absorber, (b) Comparison of S-parameters of different conditions in the PIFA antenna

6.3.2 Radiation pattern analysis

The 3D radiation patterns of the proposed MIMO PIFA at 5.65GHz frequency is presented in Figure 6.5. The radiation pattern in the case when Antenna-1 is energized while keeping Antenna-2 matched terminated is shown in Figure 6.5(a). The radiation pattern in the second case when Antenna-2 is energized while keeping Antenna-1 matched terminated is shown in Figure 6.5(b). It is noted that the radiation pattern of Antenna-1 and Antenna-2 are complementary to each other as two antennas are mirror images of one another which will help to lessen the multipath fading effect.

6.3.3 Diversity parameters analysis

It order to examine the diversity performance of the proposed MIMO PIFA structure, some important parameters like envelope correlation coefficient (ECC), mean effective gain (MEG) and effective diversity gain (EDG) are calculated and mentioned in Table 6.3. These parameters are calculated in CST MWS using far-field pattern data in the isotropic environment. The calculated value of ECC is well below a defined limit of ECC which satisfies the criteria of MIMO systems. Moreover, the MEG of Ant.-1 and Ant.-2 is referred to as MEG1 and MEG2. The calculated values of MEG1 and MEG2 are the same due to the uniform environment. Therefore their ratio is one that fulfills the equality criterion for two elements. Moreover, the calculated value of EDG is 9.99.

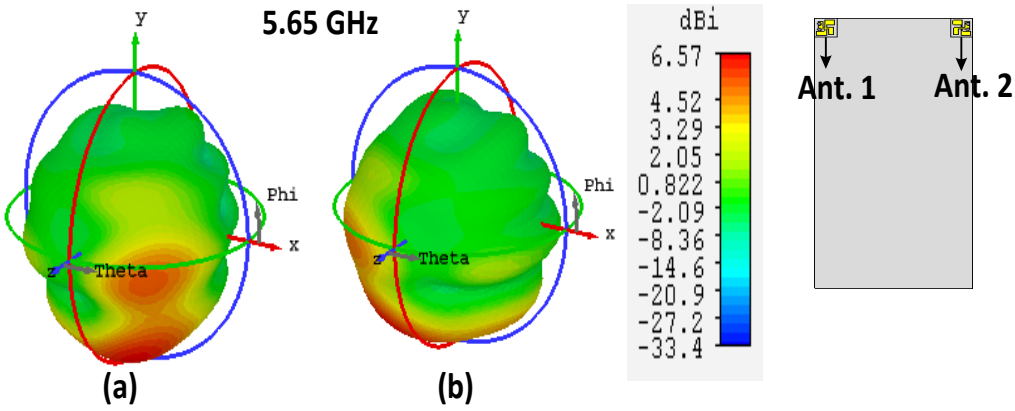

Figure 6.5 (a) 3D pattern when Antenna-1 is excited and Antenna-2 is matched terminated, (b) 3D pattern when Antenna-2 is excited and Antenna-1 is matched terminated

Table 6.3 Diversity Parameters of the Proposed PIFA

Frequency (GHz)	ECC	MEG1	MEG2	MEG Ratio	EDG
5.65	0.033	-3.01	-3.01	1	9.99

6.4 EXPERIMENTAL RESULTS

To measure the fabricated MIMO PIFA, a keysight ENA series network analyzer E5063A (100 kHz-18 GHz) is used. The front and back view of the PIFA is presented in Figure 6.6(a) and the measurement setup of the proposed PIFA structure is presented in Figure 6.6(b). The fabricated PIFA structure is connected with the series network analyzer through two ports of the PIFA with the help of cables and calibrated properly. Further, the reflection coefficient $\boldsymbol{S_{11}}$ and transmission coefficient $\boldsymbol{S_{21}}$ are measured and noted. A comparison of simulated and measured results is shown in Figure 6.6(c).

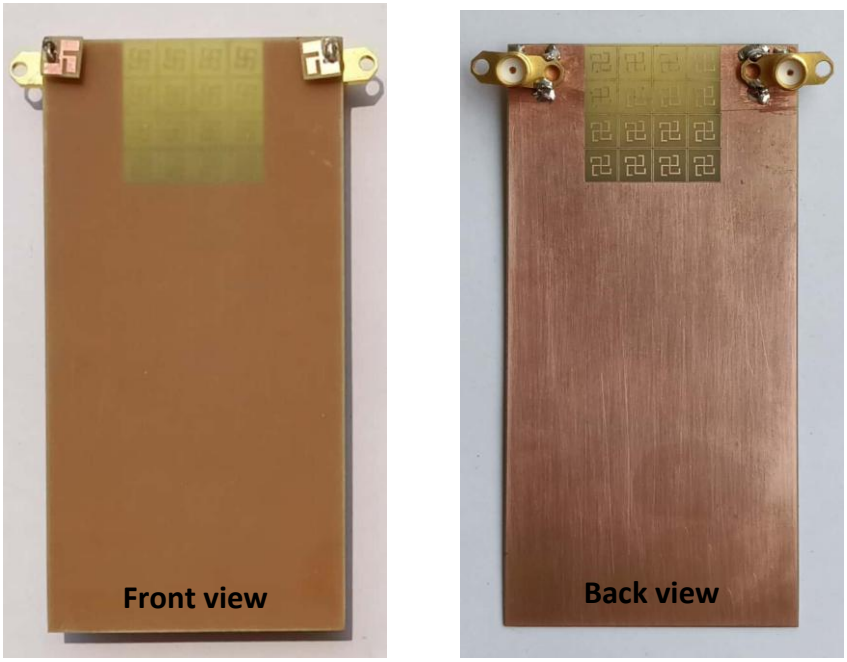

(a)

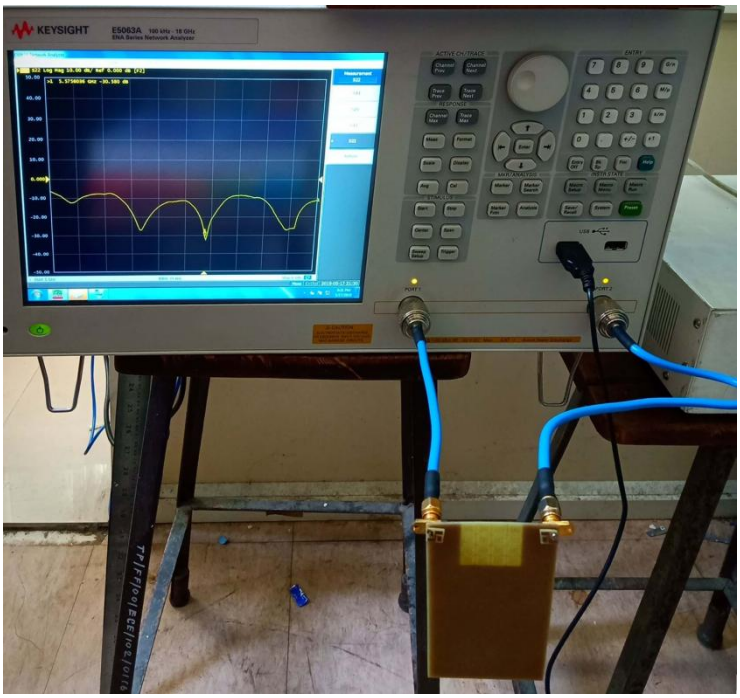

(b)

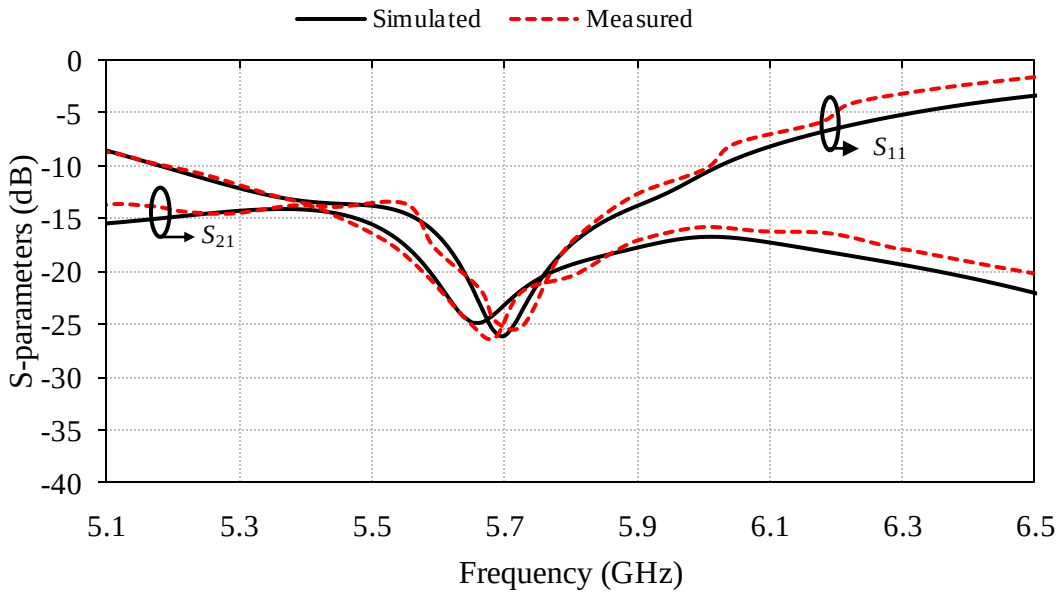

(c)

Figure 6.6 (a) Front and back view of the fabricated PIFA, (b) Measurement setup of the proposed PIFA, (c) Comparison of simulated and measured results

CHAPTER 7
CONCLUSION AND FUTURE SCOPE

7.1 CONCLUSION

Different conclusions are drawn from designs i.e. dual-band absorber design, triple-band absorber design, wideband absorber design, and MIMO PIFA design.

In this thesis, a two-band metamaterial absorber has been discussed in detail. The simulation results confirm the polarization-insensitivity of the proposed design. The unit cell dimensions of all the absorber structures are optimized to get better absorption. The simulation results show absorption frequency at 5.65 GHz and 10.91 GHz with a peak absorptivity of 98.8% and 99.5%, respectively. The compact, ultrathin, polarization-independent proposed absorber can be a high-quality candidate for C-band and X-band applications.

A triple resonance metamaterial absorber has been discussed in this thesis. The unit cell dimensions of all the absorber structures are optimized to get better absorption. The polarization independency of the projected absorber is proved by the simulation results. The simulation results show absorption frequency at 3.42 GHz, 9.61 GHz and 13 GHz with peak absorptivity of 99.59%, 99.11%, and 99.13%, respectively. The compact, ultra-thin, polarization-insensitive proposed absorber can be applied for S-band, X-band and Ku-band applications.

A wideband metamaterial absorber has been discussed in this thesis. The simulation results proved the polarization-independent behavior of the proposed wideband absorber. The unit cell dimensions of the proposed structure are optimized to get the wider bandwidth with good absorption. The simulation results show the wide band of 9 GHz from 12 GHz to 21 GHz frequency range with three resonance peaks at 12 GHz, 17 GHz and 21 GHz having peak absorptivity of 99.6%, 99.9%, and 97.6%, respectively.

Design of a planar inverted-F antenna (PIFA) with MIMO configuration has been presented for the use in mobile handsets with high isolation between the antenna components. A 4 × 4 array of metamaterial absorber is used to isolate the antenna elements and this absorber 4 × 4 array enhances the isolation between the elements without disturbing the reflection coefficient attributes. This proposed structure

provides maximum isolation of about -25dB when the absorber array is engraved at the bottom portion of the substrate within the ground plane.

7.2 FUTURE SCOPE

We can project the structure having more compactness, ultra-small thickness along with the polarization independence property. Further, we can propose a design having absorption curves more than three i.e. four absorption curves, five absorption curves, six absorption curves and many more so that it can be used for more applications. A design providing ultra-wideband absorption can also be invented. Moreover, a conformal metamaterial absorber can also be invented for the use in applications where flexible absorber designs are required. Furthermore, an antenna design with more improved isolation or resonating at multiple frequencies can also be proposed.

REFERENCES

[1] https://en.wikipedia.org/wiki/Metamaterial.

[2] Caloz C and Itoh T (2006). Electromagnetic metamaterials, transmission line theory and microwave applications, *The engineering approach, Wiley, Hoboken*, NJ, 1-352.

[3] Shelby RA, Smith DR and Schultz S (2001). Experimental verification of a negative index of refraction, *Science*, 292, 77–79.

[4] Fang N *et al*. (2005). Sub-diffraction-limited optical imaging with a silver superlens, *Science*, 308, 534–537.

[5] Schurig D *et al*. (2006). Metamaterial electromagnetic cloak at microwave frequencies, *Science*, 314, 977–980.

[6] Enoch S, Tayeb G and Vincent P (2002). A metamaterial for directive emission, *Physics Review Letter*, 89, 3901–3904.

[7] Landy NI *et al.* (2008). Perfect metamaterial absorber, *Physics Review Letter*, 100, 207402.

[8] Tao H *et al*. (2008). A metamaterial absorber for the terahertz regime, design fabrication and characterization, *Optic Express* , 16, 7181–7188.

[9] Liu X *et al*. (2010). Infrared spatial and frequency selective metamaterial with near-unity absorbance, *Physics Review Letter*, 104, 7403.

[10] Bilotti F, Nucci L and Vegni L (2006). An SRR-based microwave absorber, *Microwave Optical Technology Letters*, 48, 2171–2175.

[11] Li L, Yang Y and Liang C (2011). A wide-angle polarization-insensitive ultra-thin metamaterial absorber with three resonant modes, *Journal of Applied Physics*, 110, 063702.

[12] Cheng YZ *et al*. (2012). Design, fabrication and measurement of a broadband polarization insensitive metamaterial absorber based on lumped elements, *Journal of Applied Physics*, 111, 044902.

[13] Li MH *et al*. (2011). Ultrathin multiband gigahertz metamaterial absorbers, *Journal of Applied Physics*, 110, 014909.

[14] forum.nasaspaceflight.com/index.php?action=dlattach;topic=36313.0;attach=829404.

[15] Li MH, Yang HL and Hou X (2010). Perfect metamaterial absorber with dual bands, *Progress In Electromagnetics Research*, 108, 37-49.

[16] Li H *et al.* (2011). Ultrathin multiband gigahertz metamaterial absorbers, *Journal of Applied Physics*, 110, 014909 (1-8).

[17] Li L, Yang Y and Liang C (2011). A wide-angle polarization-insensitive ultra-thin metamaterial absorber with three resonant modes, *Journal of Applied Physics*, 110, 063702 (1-5).

[18] Shen X *et al.* (2011). Polarization-independent wide-angle triple-band metamaterial absorber, *Optics Express*, 19(10), 9041-9047.

[19] Chattha HT and Huang Y (2011). Low profile dual-feed planar inverted-F antenna for wireless LAN applications, *Microwave And Optical Technology Letters*, 53(6), 1382-1386.

[20] Kim D, Kim U and Choi J (2011). Design of a dual-band MIMO antenna for mobile wimax application, *Microwave And Optical Technology Letters*, 53(2), 410-414.

[21] Peng XY, Zhang DH and Teng JH (2012). Ultrathin multi-band planar metamaterial absorber based on standing wave resonances, *Optics Express*, 10, 27756-27765.

[22] Liu Y *et al*. (2012). Ultra-thin broadband metamaterial absorber, *Applied Physics A*, 108, 19–24.

[23] Qiu L *et al*. (2012). Transmit–receive isolation improvement of antenna arrays by using EBG structures, *IEEE Antenna and Wireless Propagation Letters*, 11, 93-96.

[24] Bhattacharyya S, Ghosh S and Srivastava KV (2013). Triple band polarization-independent metamaterial absorber with bandwidth enhancement at X-band, *Journal of Applied Physics*, 114, 094514 (1-7).

[25] Lee HM and Lee HS (2013). A metamaterial based microwave absorber composed of coplanar electric-field-coupled resonator and wire array, *Progress In Electromagnetics Research C*, 34, 111-121.

[26] Tak J, Lee Y and Choi J (2013). Design of a Metamaterial Absorber for ISM Applications, *Journal Of Electromagnetic Engineering And Science*, 13(1), 1-7.

[27] Kollatou TM *et al*. (2013). A family of ultra-thin, polarization-insensitive, multi-band, highly absorbing metamaterial structures, *Progress In Electromagnetics Research*, 136, 579-594.

[28] Bhattacharyya S, Ghosh S and Srivastava KV (2013). Bandwidth enhanced metamaterial absorber using electric field–driven LC resonator for airborne radar applications, *Microwave and Optical Technology Letters*, 55, 2131-2137.

[29] Singh HS *et al*. (2013). Low mutual coupling between mimo anten-nas by using two folded shorting strips, *Progress In Electromagnetics Research B*, 53, 205–221.

[30] Singh HS *et al*. (2013). Spiral-shaped High Isolated Monopole MIMO/Diversity Antenna for Small Mobile Terminals, *Conference on Advances in Communication and Control Systems (CAC2S)*, 612-616.

[31] Singh HS *et al*. (2013). A Compact Tri-Band MIMO/Diversity Antenna for Mobile Handsets, *IEEE CONECCT*, 1569684823, 1-6.

[32] Puri R and Singla R (2014). Design and simulation of metamaterial based resonant absorber, *International Journal of Science and Research (IJSR)*, 3, 2360-2362.

[33] Jamilan S, Azarmanesh MN and Zari D (2014). Design and characterization of a dual-band metamaterial absorber based on destructive interferences, *Progress In Electromagnetics Research C*, 47, 95-101.

[34] Ghosh S, Bhattacharyya S and Srivastava KV (2014). Bandwidth enhancement of an ultrathin polarization insensitive metamaterial absorber, *Microwave and Optical Technology Letters*, 56(2), 350-355.

[35] Puri R and Singla R (2014). Design and Simulation of Metamaterial based Resonant Absorber, *International Journal of Science and Research (IJSR)*, 3(7), 2360-2362.

[36] Bhattacharyya S *et al*. (2014). A broadband wide angle metamaterial absorber for defense applications, *IEEE International Microwave and RF Conference (IMaRC)*, 33-36.

[37] Ayop O *et al*. (2014). Dual band polarization insensitive and wide angle circular ring metamaterial absorber, *IEEE*, 978, 955-957.

[38] Wang BY *et al*. (2014). A novel ultrathin and broadband microwave metamaterial absorber, *Journal of Applied Physics*, 116, 094504 (1-7).

[39] Kollatou T, Dimitriadis AI and Antonopoulos CS (2014). Ultra-thin, polarization-insensitive, microwave metamaterial absorbers for EMC applications, *https://www.researchgate.net*, publication 244484923.

[40] Ghosh S, Bhattacharyya S and Srivastava KV (2014). Bandwidth enhancement of an ultrathin polarization insensitive metamaterial absorber, *Microwave And Optical Technology Letters*, 56(2), 350-355.

[41] Singh HS *et al*. (2014). Design of Low Profile Ultra Wideband PIFA for MIMO Applications, *IEEE Region 10 Symposium*, 978-1-4799-2027-3/14, 420-425.

[42] Yoo YJ *et al*. (2015). Triple-band perfect metamaterial absorption, based on single cut-wire bar, *Applied Physics Letters*, 106, 071105 (1-5).

[43] Zhai H *et al*. (2015). A triple-band ultrathin metamaterial absorber with wide-angle and polarization stability, *IEEE Antennas and Wireless Propagation Letters*, 14, 241-244.

[44] Bhattacharyya S *et al*. (2015). Bandwidth-enhanced dual-band dual-layer polarization-independent ultra-thin metamaterial absorber, *Applied Physics A*, 118, 207–215.

[45] Chaurasiya D *et al*. (2015). An ultra-thin triple band polarization-insensitive metamaterial absorber for C-band applications, *IEEE*, 978, 15-21.

[46] Sood D and Tripathi CC (2015). A wideband wide-angle ultra-thin metamaterial microwave absorber, *Progress In Electromagnetics Research M*, 44, 39–46.

[47] Singh HS *et al*. (2015). A low profile tri-band diversity antenna for wlan/wimax/hiperlan applications with high isolation, *Microwave And Optical Technology Letters*, 57(2), 452-457.

[48] Agrawal A, Singh A and Misra M (2016). A multiband metamaterial absorber with concentric continuous rings resonator structure, *International Journal of Advances in Microwave Technology (IJAMT)*, 1, 5-9.

[49] Bhattacharyya S, Ghosh S and Srivastva KV (2016). A microwave metamaterial absorber with wide bandwidth, *URSI Asia-Pacific Radio Science Conference*, 1215-1218.

[50] Ramya S and Rao IS (2016). Design of polarization-insensitive dual band metamaterial absorber, *Progress In Electromagnetics Research M*, 50, 23–31.

[51] Montaser AM (2016). Design of metamaterial absorber for all bands from microwave to terahertz ranges, *International Journal of Advanced Research in Electronics and Communication Engineering (IJARECE)*, 5, 1475-1481.

[52] Agarwal M and Meshram MK (2016). Isolation improvement of 5 GHz WLAN antenna array using metamaterial absorber, *URSI Asia-Pacific Radio Science Conference*, 978-1-4673-8801-6/16, 1050-1053.

[53] Kaur KP, Upadhyaya T and Palandoken M (2017). Dual-band polarization-insensitive metamaterial inspired microwave absorber for LTE-band applications, *Progress In Electromagnetics Research C*, 77, 91–100.

[54] Cheng YZ *et al*. (2017). Ultra-thin multi-band polarization-insensitive microwave metamaterial absorber based on multiple-order responses using a single resonator structure, *Materials*, 10, 1241 (1-12).

[55] Cheng YZ *et al*. (2017). Ultrathin Six-Band Polarization-Insensitive Perfect Metamaterial Absorber Based on a Cross-Cave Patch Resonator for Terahertz Waves, *Materials*, 10, 591 (1-13).

[56] Sharma SK *et al*. (2017). Ultra-thin dual-band polarization insensitive conformal metamaterial absorber, *Microwave and Optical Technology Letters*, 59(2), 348-353.

[57] Yu X, Song Y and Fan S (2017). Research on a multiband metamaterial absorber, *AIP Conference Proceedings*, 1890, 040102 (1-7).

[58] Mishra N *et al*. (2017). An investigation on compact ultra-thin triple band polarization independent metamaterial absorber for microwave frequency applications, *IEEE*, 5, 2169-3536.

[59] Mol VAL and Aanandan CK (2017). An ultrathin microwave metamaterial absorber with enhanced bandwidth and angular stability, *Journal of Physics Communications*, 1, 015003 (1-12).

[60] Thummaluru SR, Mishra N and Chaudhary RK (2017). Design and analysis of an ultrathin triple-band polarization independent metamaterial absorber, *International Journal of Electronics and Communications*, 82, 508–515.

[61] Wang J *et al.* (2018). Polarization-controlled and flexible single, penta-band metamaterial absorber, *Materials*, 11, 16-19.

[62] Fan S and Song Y (2018). UHF metamaterial absorber with small-size unit cell by combining fractal and coupling lines, *International Journal of Antennas and Propagation*, 10, 1-9.

[63] Sekar R and Inabathini SR (2018). An ultra-thin compact wideband metamaterial absorber, *Radio engineering*, 27, 1-8.

[64] Asgharian R, Zakeri B and Karimi O (2018). Modified hexagonal triple-band metamaterial absorber with wide-angle stability, *International Journal of Electronics and Communications*, https://doi.org/10.1016/j.aeue.2018.02.013, 1-12.

APPENDIX

The absorber is a sandwich of two layers made of metal and is separated by the FR-4 dielectric substrate. The top layer is having the metallic resonating structure while the bottom layer is completely laminated with copper. Full-wave simulations and optimizations of the metamaterial absorber are carried out using finite integration technique (FIT) based computer simulation microwave studio (CST MWS) with periodic boundary conditions.

Moreover, the absorptivity $A(\omega)$ of the design is calculated by Equation (9.1),

$$A(\omega) = 1 - |S_{11}(\omega)|^2 - |S_{21}(\omega)|^2 \qquad (9.1)$$

where, $S_{21}(\omega)$ and $S_{11}(\omega)$ are transmission coefficient and reflection coefficient, respectively. However, the ground plane is backed with completely metal which prevents the incident wave transmission. Hence, the transmission coefficiency will become zero i.e. $S_{21}(\omega) = 0$. Thus, absorptivity can be calculated by Equation (9.2).

$$A(\omega) = 1 - |S_{11}(\omega)|^2 \qquad (9.2)$$

ME Thesis

ORIGINALITY REPORT

20%	10%	16%	12%
SIMILARITY INDEX	INTERNET SOURCES	PUBLICATIONS	STUDENT PAPERS

PRIMARY SOURCES

1	www.jpier.org Internet Source	1%
2	Sreenath Reddy Thummaluru, Naveen Mishra, Raghvendra Kumar Chaudhary. "Design and analysis of an ultrathin triple-band polarization independent metamaterial absorber", AEU - International Journal of Electronics and Communications, 2017 Publication	1%
3	aip.scitation.org Internet Source	<1%
4	Submitted to VIT University Student Paper	<1%
5	Submitted to Universiti Kebangsaan Malaysia Student Paper	<1%
6	Submitted to Higher Education Commission Pakistan Student Paper	<1%
7	"Polar Remote Sensing", Springer Nature, 2006	

Manpreet 24/6/19

Hari Shankar Singh 24/06/2019